RAYS AND BEAMS NEAR THE SHADOW BOUNDARY

by

Weixing Gao

Thesis submitted to the Faculty of the Graduate School of
the New Jersey Institute of Technology in partial fufillment of
the requirements for the degree of
Master of Science in Electrical Engineering
1989

APPROVAL SHEET

Title of the thesis: RAYS AND BEAMS NEAR THE SHADOW BOUNDARY

Name of Candidates: Weixing Gao

Master of Science in Electrical Engineering, 1989

Thesis and Abstract Approved: _____ _____ Date

Dr. Edip Niver

Associate Professor

Electical Engineering

Signatures of the other members _____ _____ Date

of the thesis committee. _____ _____ Date

_____ _____ Date

VITA

Name: Weixing Gao

Degree and date to be confirred: M.S.E.E., 1989

Secondary education: Beijing No.101 High School, 1977

Collegiate institutions attended	Date	Degree	Date of Degree
New Jersey Inst. of Tech.	87/89	M.S.E.E.	May 1989
Beijing Institute of Posts and Telecommunications	78/82	B.S.E.E	July 1982

Major: Electrical Engineering

ABSTRACT

Title of Thesis: Rays and Beams Near the Shadow Boundary

Weixing Gao, Master of Science, 1989

Thesis directed by: Associate Professor Dr. Edip Niver

Asymptotic techniques in wave propagation problems exhibit attractive features in computational aspects compared to numerical methods. However, they experience problems in complicated environments due to the transition regions associated with them. The transition region involving a shadow boundary in the downward refractive index profile has been investigated. The ray paths were determined solving the ray equation analytically. The Green's function due to a line source is constructed and evaluated using numerical integration (reference solution) and asymptotic techniques. Then, the field produced by the source, is synthesized, using superposition of beams generated from complex source point representation. The floating parameters such as beam width, number of beams and the width of the cone were tuned to get "optimum" solution which represented the total field in a very broad region very accurately. However, difficulties were encountered as the observer moved into the shadow region, the search for complex saddle point was not successful. Another difficulty is the numerical integration of the generalized ray integral for the observer located close to the shadow boundary. It was difficult to determine the steepest descent path numerically, due to rapid growth of the integrand. Over all it was demonstrated that the complex source point generated beams could be used to construct the wave fields in the inhomogeneous media.

ACKNOWLEGEMENT

The author wishes to express special thanks to Dr. Edip Niver who provided more than enough of his share to make this thesis materialized. All statements said will be too little to represent what his efforts have been during the course of this study.

TABLE OF CONTENTS

LIST OF FIGURES

CHAPTER I INTRODUCTION

Problem arising in tropospheric or ionospheric communication systems, underwater acoustics and seismology generally involve media with varying parameters to characterize the propagation speed. Wave propagation in such an inhomogeneous environment usually requires sophisticated analytical or numerical procedures due to a complexity of wave processes taken place. The ray method [1] is one of the commonly used tools to predict response from source excited waves.

The popularity of the ray method stems from its applicability to realistic environments where experimental data leads to numerically specified profiles of refractive index or sound speed variations in longitudinal as well as transversal directions. However, search for ray paths connecting source and receiver may require many iterations to achieve specified accuracy. Though geometrical rays yield quite accurate information on trajectories of energy flow, amplitude evaluation starts to fail within transition regions where interference of two or more ray fields of different species occurs. Such transition regions in the ray method exist quite often near shadow boundaries, near critical refection, caustics, etc., where the number of ray species on one side differs from that on the other. Discontinuities in ray representations sometimes can be smoothed out with only partial success by transition functions, e.g., Airy function to correct ray fields near caustics.

One suggested alternative is to replace these transitional rays with equivalent modes and remainders [2]. Furthermore, hybrid ray-mode methods have been extended to an inhomogeneous medium to take

advantages of asymptotic ray theory where ever it applies and the remaining spectral void is filled with modes and remainders [2]. This scheme furnishes some basic insights into the propagation mechanisms and works effectively in analytical test profiles. It remains to be extended to more general environments, especially those specified numerically instead of analytically. Recently, an asymptotic procedure based on the superposition of the Gaussian beams for the computation of wave fields in an inhomogeneous medium is proposed [3]. The attractive features of the Gaussian Beam Method (GBM) are inherent in the uniform nature of beam solutions in transition regions and the elimination of the search for ray paths. GBM is based on shooting stack of beams from the source in the direction of the receiver. The beam axis propagates along the ray paths which now do not require a 2-point search. The parabolic wave equation method gives solutions of the wave equation concentrated close to these central rays in terms of the Gaussian beams. The wave field is then determined at any point as a superposition of individual Gaussian beams passing through the vicinity of the receiver.

The parabolic wave equation was initially applied to radio wave propagation problems by Fock and Leontonovich [5]. Later it was applied to other wave problems, i.e., acoustics [6] and seismology [7]. It was first applied to the solution of the wave equation concentrated close to rays by Babich and his co-workers [8-10].

Babich and Pankratova [10] originally suggested to describe the wave field in the high frequency region by means of an integral over all beams concentrated close to the rays and used this integral for mathematical investigations. Based on this paper, Popov [12] suggested a new method now known as the Gaussian Beam Method (GBM).

Results of the first attempts of using this method for computation of seismic wave fields in a 2-D inhomogeneous medium was initiated by Popov, Psencik and Cerveny [4]. Later on the method is extended to other problems by Cerveny & Psencik [13], in Czechoslovakia and a group of researchers in MIT [14-16]. The common deficiency in the published results is that no systematic approach in determination of the various parameters of the GBM exists.

The GBM has been extended to underwater acoustics [16,17] involving inhomogeneous profiles. Results were obtained using paraxial Gaussian beams and clearly evident that further work was necessary to put GBM into a systematic algorithm with a priori predictability.

The improvement developed in this thesis is to use beam expressions obtained from complex source point representations [18-19] rather than their paraxial approximations that were used before. Results are compared to the reference solution obtained by numerical integration of the Green's function for the downward sloping profile which involves the shadow boundary if asymptotic ray method is used.

CHAPTER II. MODEL CONFIGURATION AND GEOMETRICAL RAY PATHS

The inhomogeneous medium considered in this thesis will be based on a strong downward refraction profile considered by Pedersen and Gordon [21]. This profile exhibits strong de-focusing effects with range and serves as a good example for a transition region involving the shadow boundary. The numerical treatment of this profile using paraxial Gaussian beams have been reported by Porter and Bucker [16].

A. WAVE EQUATION

The wave equation for an inhomogeneous medium is

$$\nabla^2 u + k_0^2 n^2(r)\, u = 0 \qquad (2\text{-}1)$$

where k_0 is the wave number in free space. $n(r)$ is the refractive index of the inhomogeneous medium. It is a non-negative real function of position.

In this thesis, two dimensional geometry is considered where medium variation will depend on the coordinate y as

$$n^2(y) = N_1^2(1 + qy) \qquad (2\text{-}2)$$

where N_1 and q are positive constants. Fig.1 shows the refractive index profile when $N_1=1$, $q=1.4650\times10^{-3}$. The units are chosen according the notation used by Porter and Bucker [16].

The 2-D wave equation now can be expressed as

$$\left[\frac{\partial^2}{\partial x^2} + \frac{\partial^2}{\partial y^2} + k_0^2 N_1^2(1 + qy)\right] u = 0 \qquad (2\text{-}3)$$

where the variable u may represent a pressure in an acoustic field or an electric (magnetic) field intensity in an electromagnetic field depending on the chosen polarization.

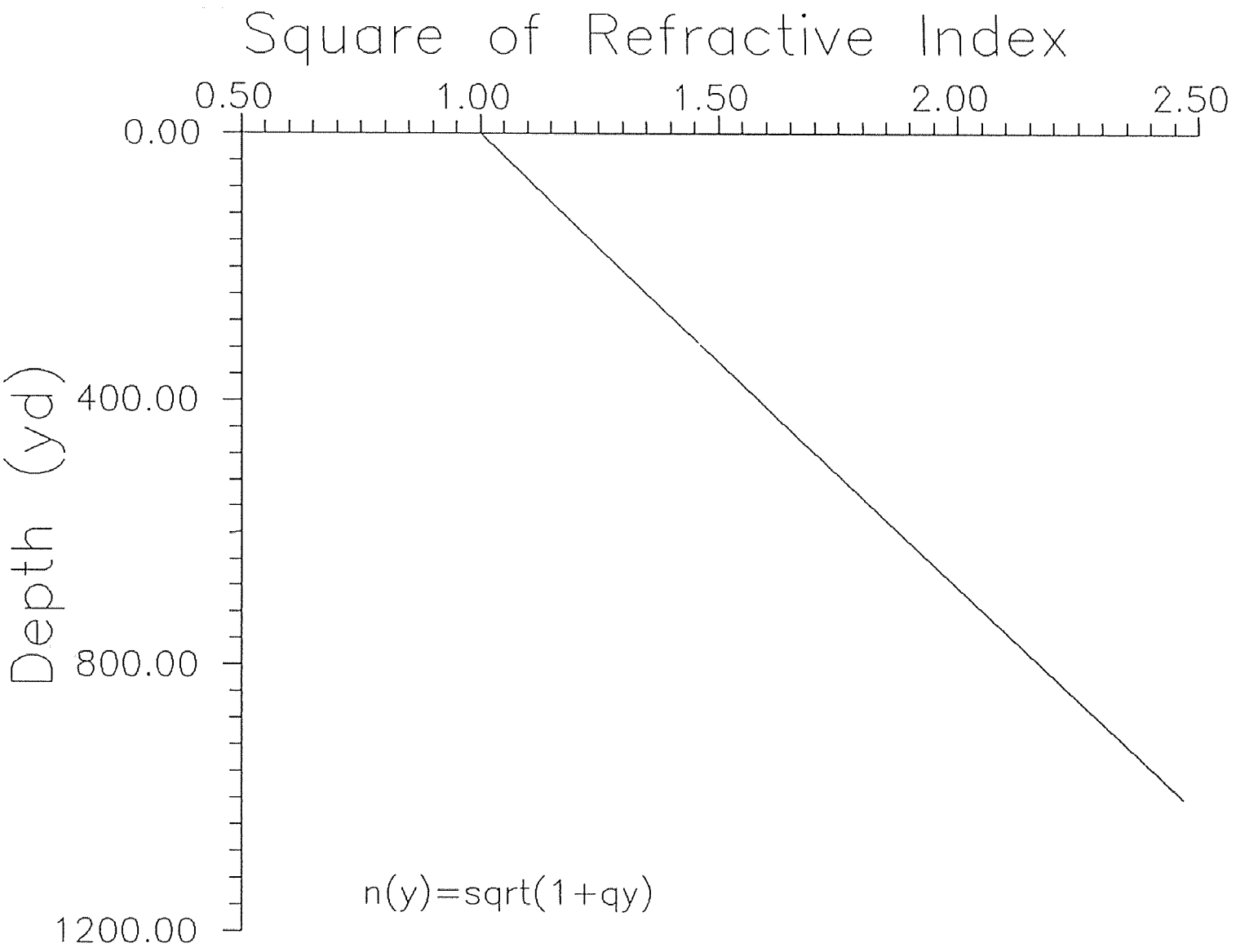

Fig.1 Refractive index variation with depth.

B. GEOMETRICAL RAY PATHS

To get the ray trace in an inhomogeneous medium characterized by $n^2(y) = N_1^2(1+qy)$, one can start from the ray equation [1].

$$\nabla\, n(r) = \frac{d}{ds}[\bar{S}(r)\, n(r)] \tag{2-4}$$

where

$$\begin{aligned} &n(r) = n(y) = \sqrt{1+qy} \\ &\bar{S}(r) = \frac{d\bar{r}}{ds} \\ &d\bar{r} = \hat{x}\,dx + \hat{y}\,dy \\ &ds = \sqrt{dx^2 + dy^2} = \sqrt{1+(\frac{dy}{dx})^2}\,dx \end{aligned} \tag{2-5}$$

One can get

$$\nabla_{xy} n(r) = \nabla_{xy} n(y) = \nabla_{xy}\sqrt{1+qy} = 0\hat{x} + \frac{q/2}{\sqrt{1+qy}}\hat{y} \tag{2-6}$$

and

$$\frac{d}{ds}\left[\,\bar{S}(r)n(r)\,\right] = \frac{d}{ds}\left[\frac{\hat{x}\,dx + y d\hat{y}}{\sqrt{1+(\frac{dy}{dx})^2}\,dx}(\sqrt{1+qy})\right]$$

Comparing equations in (2-5) and (2-6), one gets

$$\frac{d}{ds}\left[\frac{\sqrt{1+qy}}{\sqrt{1+(\frac{dy}{dx})^2}}\hat{x}\right] = 0\hat{x} \tag{2-7}$$

which implies

$$\frac{\sqrt{1+qy}}{\sqrt{1+(\frac{dy}{dx})^2}} = c_1 \tag{2-8}$$

Further, simplification results in

$$c(1+qy) = (\frac{dy}{dx})^2 + 1 \tag{2-9}$$

which leads to

$$\frac{dy}{dx} = \pm\sqrt{c(1+qy)-1} \tag{2-10}$$

Final integration yields

$$x = \int \frac{\pm\, dy}{\sqrt{c(1+qy)-1}} = \int \frac{\pm\, dy}{\sqrt{cqy + c - 1}} \tag{2-11}$$

Let $a=cq$, $b=c-1$, then

$$x=\int\frac{\pm dy}{\sqrt{ay+b}} \tag{2-12}$$

So, for $x>0$:

$$x=\int\frac{1/ad\ (ay+b)}{\sqrt{ay+b}}=\frac{2}{b}\sqrt{ay+b}+d \tag{2-13}$$

$$x=\frac{2}{cq}\sqrt{c(1+qy)-1}+d \tag{2-14}$$

Then rearrangement yields

$$(x-d)^2=\frac{4}{c^2q^2}\left[c(1+qy)-1\right] \tag{2-15}$$

After simplification

$$c(1+qy)-1=\frac{c^2q}{4}(x-d)^2$$

one obtains the ray trace expression for $0<x<x_1$, where x_1 is the location of reflection from the boundary for a ray with a given initial condition.

$$y=\frac{c_0q}{4}(x-d_0)^2+\frac{(1-c_0)}{c_0q} \tag{2-16}$$

For $0<x<x_1$, with initial conditions at $x=x_0=0$, $y=y_0$, θ_0 , one can solve for constants c_0 and d_0 as:

$$y_0=\frac{c_0q}{4}d_0+\frac{(1-c_0)}{c_0q} \tag{2-17}$$

$$tg\theta_0=\left.\frac{dy}{dx}\right|_{x=0}=\left.\frac{c_0q}{2}(x-d_0)\right|_{x=0}=\frac{c_0q}{2}d_0 \tag{2-18}$$

then,

$$d_0=\frac{2tg\theta_0}{c_0q}$$

and

$$c_0(1+qy_0)=tg^2\theta_0+1$$

They further reduce to

$$c_0 = \frac{1}{(1+qy_0)\cos\theta_0} \tag{2-19}$$

and

$$d_0 = \frac{1}{q}(1+qy_0)\sin 2\theta_0 \tag{2-20}$$

Now, one can solve for x_1 at $y=0$:

$$(x_1 - d_0) = \pm\frac{2}{c_0 q}\sqrt{c_0 - 1}$$

Since $x_1 < d_0$, (-) sign is chosen leading to

$$x_1 = d_0 - \frac{2}{c_0 q}\sqrt{c_0 - 1} \tag{2-21}$$

and the angle for reflection at x_1 is

$$tg\theta_1 = \left.\frac{dy}{dx}\right|_{x=x_1} = \frac{c_0 q}{2}(x_1 - d_0) \tag{2-22}$$

Hence, x_1 and θ_1 will be the initial conditions for the reflected ray.

Now for $x > x_1$, one can express the reflected ray path as:

$$y = \frac{c_1 q}{4}(x-d_1)^2 + \frac{(1-c_1)}{c_1 q} \tag{2-23}$$

Constants c_1 and d_1 are obtained by letting $y=0$ and $x=x_1$

$$d_1 = x_1 + \frac{2}{c_1 q}\sqrt{c_1 - 1}$$

and

$$\left.\frac{dy}{dx}\right|_{x=x_1} = \frac{c_1 q}{2}(x_1 - d_1) = tg\theta_1$$

Then

$$c_1 = tg^2\theta_1 + 1 = \frac{1}{\cos^2\theta_1} \tag{2-24}$$

and

$$d_1 = x_1 + \frac{1}{q}\sin 2\theta_1 \tag{2-25}$$

By using equation (2-16), (2-19), (2-20), (2-21), (2-22), (2-23), (2-24), (2-25), one can evaluate the ray path in a 2-D space. Fig.2 shows the ray path for the source located at 1000 yards with initial incident angle varying between $10^\circ < \theta_0 < 80^\circ$, $q = 1.4650 \times 10^{-3}$.

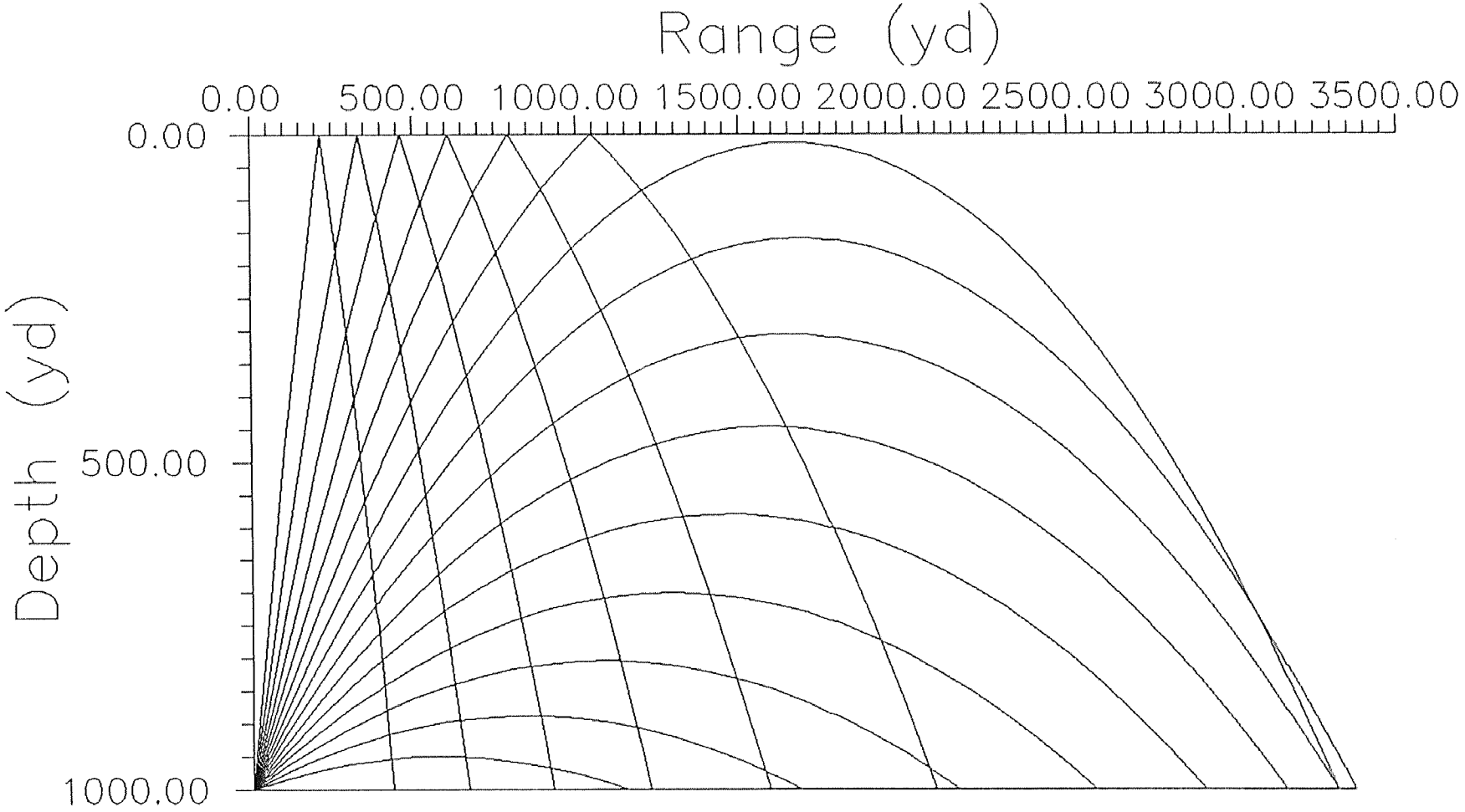

Fig.2 Ray paths for the source located at a depth of 1000 yards.

CHAPTER III. GREEN'S FUNCTION FOR THE DOWN REFRACTIVE LINEAR PROFILE

The line source is located at a distance $y=y_0$ from the boundary in an inhomogeneous medium. This geometry could simulate the underwater acoustic source in an ocean with the boundary corresponding to the surface of the ocean, or may represent the TM polarized wave excited by a magnetic line source in a tropospheric antiduct. The electromagnetic field can be determined via the Green's function, which satisfies the 2-D time-harmonic wave equation ($e^{j\omega t}$ time variation is suppressed). The following derivation for the linear profile is based on the previous work of Jones [22].

$$\left[\nabla^2 + k_0^2 n^2(y)\right] G(x,x_0,y,y_0) = -\delta(x - x_0)\,\delta(y - y_0) \tag{3-1}$$

where the Laplacian operator is

$$\nabla^2 = \frac{\partial^2}{\partial x^2} + \frac{\partial^2}{\partial y^2}$$

and refraction index varies linearly with depth,

$$n^2(y) = N_1^2(1+qy)$$

By using Fourier transfer relation for δ-function

$$\delta(x - x_0) = \frac{k_0 N_1}{2\pi} \int_{-\infty}^{+\infty} (e^{jk_0 N_1 w x_0})\, e^{-jk_0 N_1 w x}\, dw \tag{3-2}$$

The Green's function can be represented in spectral domain as

$$G(x,x_0,y,y_0) = kN_1 \int_{-\infty}^{+\infty} g(y,y_0,w)\, e^{-jk_0 N_1 w x}\, dw \tag{3-3}$$

Hence, the original 2-D representation of $G(x,x_0,y,y_0)$ may be changed into 1-D spectral form of $g(y,y_0;w)$.

Further substitution of spectral representation (3-3) into the wave equation (3-1) yields

$$\left[\frac{d^2}{dy^2}+k_0^2N_1^2(1+qy-w^2)\right]g(y,y_0;w)(2\pi e^{-jk_0N_1wx_0})=-\delta(y-y_0) \qquad (3\text{-}4)$$

Let

$$g_1(y,y_0;w) = g(y,y_0;w)\ (2\pi\ e^{-jk_0N_1wx_0})$$

which leads to

$$\left[\ \frac{d^2}{dy^2}\ +\ k_0^2N_1(1+qy-w^2)\ \right]g_1\ =\ -\delta(y-y_0) \qquad (3\text{-}5)$$

Now, let

$$Y=\alpha_1 y-\alpha_2$$

then it follows

$$\frac{d^2}{dy^2}=\frac{d^2g_1}{dY^2}\left[\frac{dY}{dy}\right]^2$$

After observing

$$\frac{dY}{dy}\ =\ \alpha_1\ ,\ \left[\ \frac{dY}{dy}\ \right]^2=\ \alpha_1^2$$

and

$$n^2(y)=N_1^2\left[1+\frac{\alpha_2}{\alpha_1}q+\frac{q}{\alpha_1}Y\right]$$

Then (3-5) yields

$$\left[\ \frac{d^2}{dy^2}\ +\ k_0^2\ N_1(1+qy-w^2)\ \right]\ g_1$$
$$=\ \left[\ \alpha_1\ \frac{d^2}{dY^2}\ +\ k_0^2\ N_1^2\ \left[\ 1+\frac{\alpha_2}{\alpha_1}q+\frac{q}{\alpha_1}Y-w^2\ \right]\ \right]\ g_1$$

Using the integral representation of the δ-function

$$\delta(y\ -\ y_0)\ =\ \frac{1}{2\ \pi}\int_{-\infty}^{+\infty}e^{-j(y-y_0)t}\ dt$$
$$=\ \frac{1}{2\ \pi}\int_{-\infty}^{+\infty}e^{-jt\left(\frac{Y+\alpha_2}{\alpha_1}-\frac{Y_0+\alpha_2}{\alpha_1}\right)}\ dt$$

Further simplification leads to

$$\delta(y-y_0) = \frac{1}{2\pi}\int_{-\infty}^{+\infty}\alpha_1 e^{-j(Y-Y_0)\frac{t}{\alpha_1}}\, d\left[\frac{t}{\alpha_1}\right] = \alpha_1\delta(Y-Y_0)$$

Then one can get:

$$\left[\frac{d^2}{dY^2} + \frac{k_0^2 N_1}{\alpha_1^2}\left[1+\frac{\alpha_2}{\alpha_1}q+\frac{q}{\alpha_1}Y-w^2\right]\right] g_1 = -\frac{1}{\alpha_1}\delta(Y-Y_0)$$

Let

$$\frac{k_0^2 N_1^2}{\alpha_1^2}\left[1+\frac{\alpha_2}{\alpha_1}q-w^2\right] = 0$$

and

$$\frac{k_0^2 N_1^2 q}{\alpha_1^3} = 1$$

Then,

$$\alpha_1 = k^{2/3}N_1^{2/3}q^{1/3} = \kappa^{2/3}q$$

and

$$\alpha_2 = \frac{\alpha_1}{q}(w^2-1) = \left[\frac{k_0 N_1}{q}\right]^{2/3}(w^2-1) = \kappa^{2/3}(w^2-1)$$

where $\kappa = \dfrac{k_0 N_1}{q} = \dfrac{2\pi f}{c_0 q}$

So, equation (3-4) can be written as:

$$\left[\frac{d^2}{dY^2} + Y\right] g(Y,Y_0)\ (2\pi e^{-jk_0 N_1 w x_0}) = -\frac{1}{\alpha_1}\delta(Y-Y_0)$$

where

$$Y = \alpha_1 y - \alpha_2 = \kappa^{2/3}(1+qy-w^2)$$

and

$$\alpha_1 = \kappa^{2/3}q$$

and

$$\alpha_2 = \kappa^{2/3}(w^2-1)$$

If we let

$$g_0(Y,Y_0) = 2\pi\alpha_1 e^{-jk_0 N_1 w x_0} g(Y,Y_0)$$

then one can get

$$\left[\frac{d^2}{dY^2} + Y \right] g_0(Y,Y_0) = -\delta(Y-Y_0) \qquad (-\alpha_2 < Y < \alpha_1 y_0 - \alpha_2)$$

where

$$Y=\alpha_1 y-\alpha_2 \ , \ Y_0=\alpha_1 y-\alpha_2$$

Now, one can construct the Green's function g_0.

When $Y \neq Y_0$

$$\frac{d^2}{dY^2} g_0 + Y g_0 = 0$$

The possible solutions $Ai(Ye^{j\pi/3})$, $Ai(Ye^{-j\pi/3})$, $Ai(Ye^{j\pi})$ represent outgoing, incoming and standing waves, respectively.

Then, one can assume the following combination for the Green's function

$$g_0(Y,Y_0) = A\left[Ai(Ye^{-j\pi/3}) + Ru\ Ai(Ye^{j\pi/3}) \right] \qquad (-\alpha_2 < Y < Y_0)$$

and (3-6)

$$g_0(Y,Y_0) = B\ Ai(Ye^{j\pi/3}) \qquad (Y < Y_0)$$

with unknown coefficients A, B and Ru.

Applying boundary condition at $Y=-\alpha_2$ (which physically corresponds to $y=0$)

$$\left. \frac{\partial g_0}{\partial Y} \right|_{Y=-\alpha_2} = 0 \qquad (3\text{-}7)$$

Applying differentiation of (3-6) to (3-7)

$$g_0'(-\alpha_2,Y_0)=A\left[Ai'(Ye^{j\pi/3})e^{-j\pi/3}+Ru\ Ai'(Ye^{j\pi/3})e^{j\pi/3}\right]=0$$

one can define the reflection coefficient Ru as

$$Ru = \left. \frac{Ai'(Ye^{-j\pi/3})\ e^{-j\pi/3}}{Ai'(Ye^{j\pi/3})\ e^{j\pi/3}} \right|_{Y=-\alpha_2} = \frac{e^{j\pi/3}\ Ai'\{\kappa^{2/3}(1-w^2)e^{-j\pi/3}\}}{Ai'\{\kappa^{2/3}(1-w^2)e^{j\pi/3}\}}$$

Extending the continuity conditions at the source location

$$g_0 \Big| Y = Y_0^+ \; = g_0 \Big| Y = Y_0^-$$

and

$$\frac{dg_0}{dy}\Big| Y = Y_0^+ \; - \frac{dg_0}{dy}\Big| Y = Y_0^- = -1$$

results in a set of simultaneous linear equations:

$$BAi(Ye^{j\pi/3}) = A\left[Ai(Y_0 e^{-j\pi/3}) + RuAi(Y_0 e^{j\pi/3})\right]$$

and

$$BAi'(Ye^{j\pi/3}) - A\left[Ai'(Y_0 e^{-j\pi/3})e^{-j\pi/3} + RuAi'(Y_0 e^{j\pi/3})e^{j\pi/3}\right] = -1$$

Solution for A yields

$$A = \frac{Ai(Y_0 e^{j\pi/3})}{e^{-j\pi/3}\, Ai'(Y_0 e^{-j\pi/3})\, Ai(Y_0 e^{j\pi/3}) - Ai(Y_0 e^{-j\pi/3})\, Ai'(Y_0 e^{j\pi/3})\, e^{j\pi/3}}$$

one can recognize the denominator as a Wronskian, hence

$$A = \frac{-\, Ai(Y_0 e^{j\pi/3})}{W\,\{\, Ai(Y_0 e^{-j\pi/3}),\; Ai(Y_0 e^{j\pi/3})\,\}}$$

Applying Wronskian for Airy function of two different components

$$W\{Ai(ze^{j2\pi/3}), Ai(ze^{-j2\pi/3})\} = \frac{j}{2\pi}$$

where $z = Y_0 e^{j\pi}$ yields the solution

$$A = 2\pi j Ai(Y_0 e^{j\pi/3})$$

Then one can express

$$g_0(Y, Y_0) = \frac{e^{jk_0 N_1 w\, x_0}}{2\pi\, \alpha_1}\, g_0(Y, Y_0) \qquad (-\alpha_2 < Y < Y_0)$$

$$= \frac{j}{\alpha_1} Ai(Y_0 e^{j\pi/3}) \left[\, Ai(Y_0 e^{-j\pi/3}) + \frac{e^{j\pi/3}\, Ai'(-\alpha_1 e^{-j\pi/3})}{Ai'(-\alpha_1 e^{j\pi/3})}\, Ai(Ye^{j\pi/3}) \,\right] e^{jk_0 N_1 w x_0}$$

where

$$\alpha_1 = \kappa^{2/3} q \;,\quad \alpha_2 = \kappa^{2/3}(w^2 - 1)$$

and

$$Y=\alpha_1 y-\alpha_2=\kappa^{2/3}(1+qy-w^2) \quad , \quad Y_0=\alpha_1 y_0-\alpha_2=\kappa^{2/3}(1+qy_0-w^2)$$

Following the notation for the spectral representation of the Green's function for $0<y<y_0$

$$G(x,x_0,y,y_0) = \int_{-\infty}^{+\infty} g(y,y_0;w)\ e^{-jk_0 N_1 wx}\ dw$$

the explicit expression for $0<y<y_0$ becomes

$$G(x,x_0,y,y_0)=\frac{k_0 N_1 j}{k^{2/3} N_1^{2/3} q^{1/3}}\int_{-\infty}^{+\infty} Ai\{\kappa^{2/3}(1+qy_0-w^2)e^{j\pi/3}\}\left[Ai\{\kappa^{2/3}(1+qy-w^2)e^{-j\pi/3}\}\right.$$
$$\left.+Ru\ Ai\{\kappa^{2/3}(1+qy-w^2)e^{j\pi/3}\}\right]\ e^{-jk_0 N_1 w(x-x_0)}\ dw \qquad (3\text{-}8)$$

Further substitution of the explicit expression for Ru into the above integral results in

$$G(x,x_0,y,y_0) =$$
$$j\kappa^{1/3}\int_{-\infty}^{+\infty}\left[Ai\{\kappa^{2/3}(1+qy-w^2)e^{j\pi/3}\}Ai\{\kappa^{2/3}(1+qy-w^2)e^{-j\pi/3}\}\right.$$
$$+\frac{e^{j\pi/3}\ Ai'\{\kappa^{2/3}(1+w^2)e^{j\pi/3}\}}{Ai'\{\kappa^{2/3}(1+w^2)\ e^{j\pi/3}\}}Ai\{\kappa^{2/3}(1+qy\ -w_0^2)e^{j\pi/3}\}$$
$$\left.Ai\{\kappa^{2/3}(1+qy-w^2)e^{-j\pi/3}\}\right]e^{-jk_0 N_1 w(x-x_0)}dw \qquad (3\text{-}9)$$

CHAPTER IV. EVALUATION OF THE GREEN'S FUNCTION

The terms in the spectral representation of the Green's function in (3-9) represent direct and reflected wave fields in the downward refractive medium. Numerical integration is not practical due to rapid oscillations of the integrand along the real axis. However at higher frequencies, the dominant contributions to the integral are mainly due to wave interferences along the specific direction. This can be mapped into w-plane as a stationary point in the phase of the integrand. Hence, the presence of a such stationary point will permit asymptotic evaluation of the integral along the steepest descent path (SDP). The two separate terms in the Green's function will be treated separately as

$$G_1 = j\kappa^{1/3}\int_{-\infty}^{+\infty} Ai\{\kappa^{2/3}(1+qy_0+w^2)e^{j\pi/3}\}\ Ai\{\kappa^{2/3}(1+qy+w^2)e^{-j\pi/3}\} \\ e^{-j\kappa q w (x-x_0)}\, dw \qquad (4\text{-}1)$$

and

$$G_2 = j\kappa^{1/3}\int_{-\infty}^{+\infty} \frac{e^{j\pi/3}Ai'\{\kappa^{2/3}(1-w^2)e^{-j\pi/3}\}}{Ai'\{\kappa^{2/3}(1-w^2)e^{j\pi/3}\}} Ai\{\kappa^{2/3}(1+qy_0-w^2)e^{j\pi/3}\} \\ Ai\{\kappa^{2/3}(1+qy-w^2)e^{j\pi/3}\}\ e^{-j\kappa q w (x-x_0)}\ dw \qquad (4\text{-}2)$$

Here, the first term G_1 represents the wave field corresponding to the direct ray and the second term G_2 represents the wave field contribution reflected form the boundary.

A. ASYMPTOTIC EVALUATION OF THE GREEN'S FUNCTION

To evaluate the Green's function by asymptotic technique, the integrand has to be expressed explicitly in terms of amplitude and phase functions. One can use the asymptotic expressions for Airy

functions [23] for $|z|$ large.

$$Ai(z) \cong \frac{exp(-\frac{2}{3} z^{3/2})}{2\pi^{1/2} z^{1/4}}$$

and

$$Ai'(z) \cong \frac{z^{1/4} exp(-\frac{2}{3} z^{3/2})}{2\pi^{1/2}} \quad (|argz| < \pi) \tag{4-3}$$

Then one can simplify the expression for Ru in (3-8) as

$$Ru = e^{j\pi/3} exp\{j\kappa 4/3(1-w^2)^{3/2}\}$$

Using the asymptotic representation, the integrand of the first term in (4-1) simplifies into

$$G_1 = \frac{j}{4\pi} \int_{-\infty}^{+\infty} \frac{e^{j\kappa\{-2/3(1+qy_0-w^2)^{3/2} + 2/3(1+qy-w^2)^{3/2} - qw(x-x_0)\}}}{4\pi (1+qy_0-w^2)^{1/4} (1+qy-w^2)^{1/4}} dw \tag{4-4}$$

Using the stationary phase method, the integral in (4-4) can be approximated as

$$G_1 \cong \sqrt{\frac{2\pi}{\kappa Q_1''(w_{s1})}} F_1(w_{s1}) e^{j\kappa Q_1(w_{s1})} \tag{4-5}$$

where only the leading term is kept. Here, the phase function

$$Q_1(w) = \{-2/3(1+qy_0-w^2)^{3/2} + 2/3(1+qy-w^2)^{3/2} - qw\ (x-x_0)\}$$

has a stationary point determined by the condition

$$Q'(w_{s1}) = \{2w_{s1}(1+qy_0-w_{s1}^2)^{1/2} - 2w_{s1}(1+qy-w_{s1}^2)^{1/2} - q(x-x_0)\} = 0$$

The stationary point w_{s1} corresponds to a saddle point located on the SDP. The saddle point is determined numerically. Fig.3 clearly indicates the presence of valley and mountain regions surrounding the saddle point.

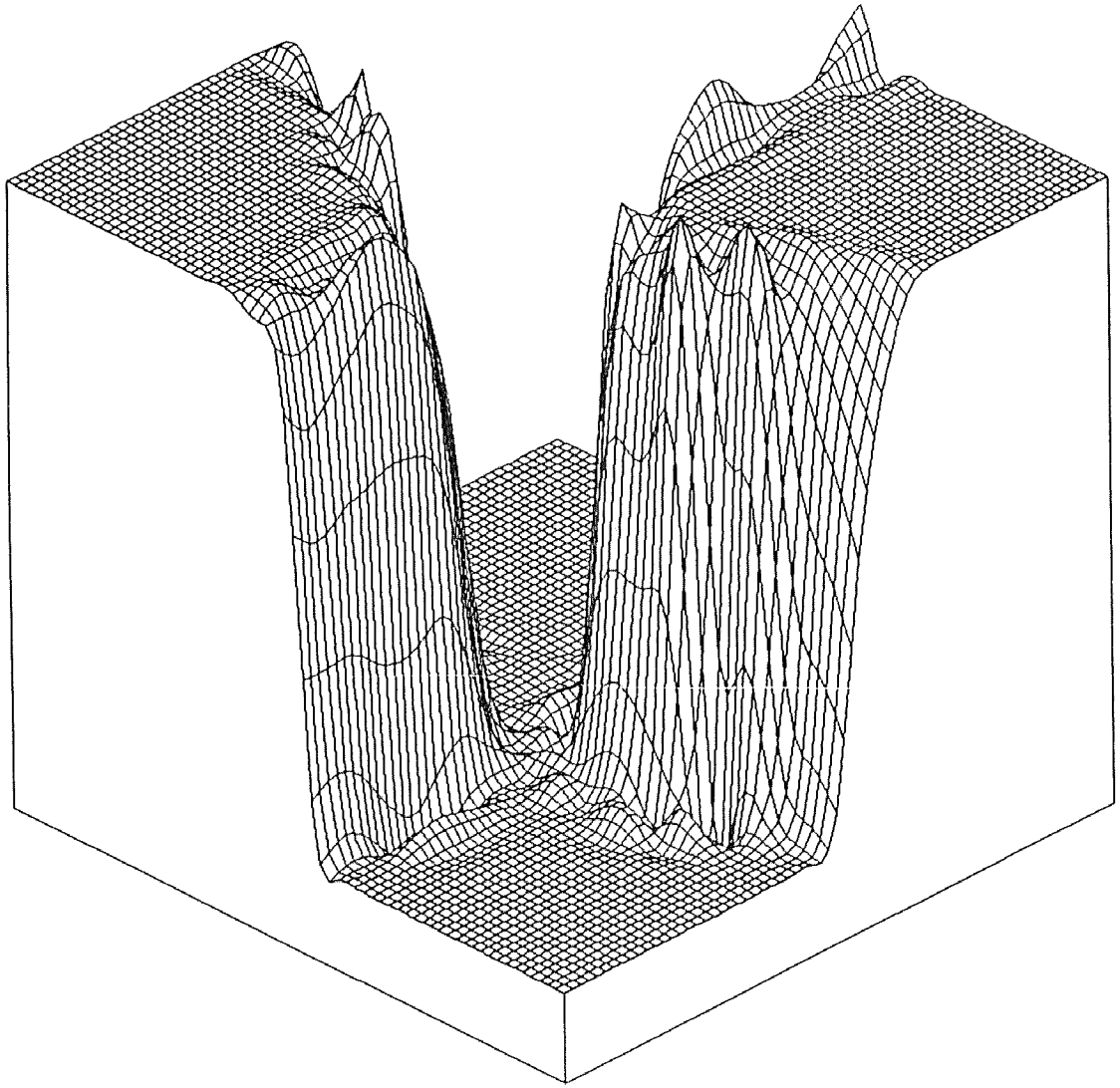

Fig.3 Saddle point of direct ray (ART)

The amplitude in (4-5) consists of

$$Q_1''(w)=\{2(1+q y_0-w^2)^{1/2}-2w^2(1+q y-w^2)^{-1/2}\}$$
$$-\{2(1+qy-w^2)^{1/2}-2w^2(1+qy-w^2)^{1/2}\}$$

and

$$F_1(w)=\frac{j}{4\pi\ (1+q y_0-w^2)^{1/4}(1+qy-w^2)^{1/4}}$$

Similarly, the reflected wave field can be evaluated as the direct ray. The asymptotic evaluation of the integrand in (4-2) yields

$$G_2=\frac{j}{4\pi}\int_{-\infty}^{+\infty}\frac{e^{jk\{-2/3(1+qy_0-w^2)^{3/2}-2/3(1+qy-w^2)^{3/2}+4/3(1-w^2)^{3/2}-qw(x-x_0)}}{(1+qy_0-w^2)^{1/4}(1+q y-w^2)^{1/4}}dw$$

Again, by stationary phase method, one gets the reflected ray contribution as

$$G_2 \cong \sqrt{\frac{2\pi}{\kappa\ Q_2''(w_{s2})}}\ F_2(w_{s2})\ e^{j\kappa Q_2(w_{s2})} \qquad (4\text{-}6)$$

where the saddle point w_{s2} is determined by

$$Q'(w_{s2})=\{2w(1+qy_0-w_{s2}^2)^{1/2}+2w_{s2}(1+qy-w_{s2}^2)^{1/2}-4w_{s2}(1-w_{s2}^2)^{1/2}-q(x-x\ )\}=0$$

The phase and amplitude in (4-6) is determined by

$$Q_2(w)=\{-2/3(1+qy_0-w^2)^{3/2}-2/3(1+qy-w^2)^{3/2}+4/3(1-w^2)^{3/2}-qw(x-x_0)\}$$

and

$$Q_2''(w)\ =\ \{2(1+q y_0-w^2)^{1/2}-2w^2(1+qy_0-w^2)^{-1/2}\}\ +\ \{2(1+qy-w^2)^{1/2}$$
$$-2w^2(1+qy-w^2)^{-1/2}\}\ -\ \{4(1-w^2)^{1/2}-4w^2(1-w^2)^{-1/2}\}$$

and

$$F_2(w)\ =\ \frac{j}{4\pi\ (1+q y_0-w^2)^{1/4}(1+qy-w^2)^{1/4}}$$

Finally, the asymptotic expression of the Green's function can be expressed as a superposition of the direct and reflected rays

$$G(x,x_0,y,y_0)=\sqrt{\frac{2\pi}{\kappa\ Q_1(w_{s1})}}F(w_{s1})e^{j\kappa Q_1(w_{s1})}+\sqrt{\frac{2\pi}{\kappa\ Q_2(w_{s2})}}F(w_{s2})e^{j\kappa Q_2(w_{s2})} \qquad (4\text{-}7)$$

B. NUMERICAL INTEGRATION OF THE GENERALIZED RAY

Asymptotic Ray Theory (ART) represented by (4-7) begins to fail as

the observer starts to move toward the shadow boundary of Fig.2. The region further away from the boundary experiences only the direct ray where as the region between the shadow boundary and the source is being illuminated by both direct and reflected rays. The failure of the ART to represent the total field in the transition region and beyond requires an alternative approach. The reference solution to check the validity of ART wherever it applies is to integrate the Green's function without referring to asymptotic approximations.

However, as was mentioned before, numerical integration along the real axis is highly difficult and time consuming. The deformation of the integration contour from the real axis will permit more efficient evaluations due to rapid decay of the integrand along the SDP as shown in Fig.4.

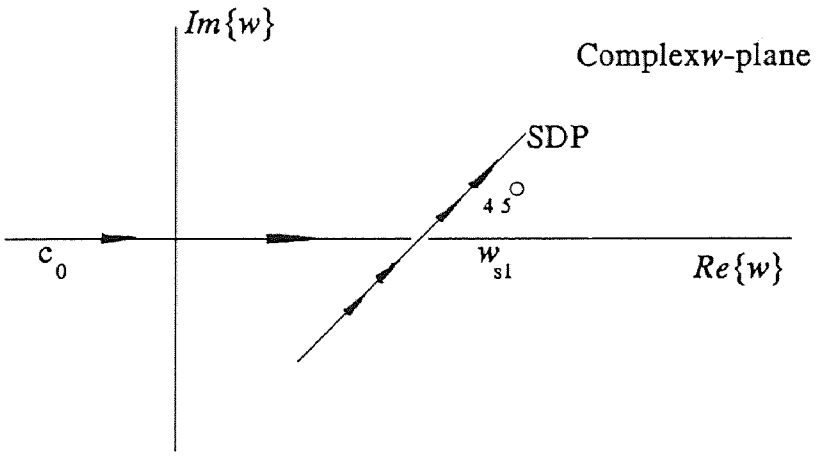

Fig.4 Deformed integration contour along the SDP.

Such a path can be found approximately [2] by employing asymptotic approximations for the functions in the integrand as in (4-5) and (4-6).

After locating the saddle point, search in the vicinity for region in complex w-plane where in the integrand decays. Starting from a

saddle point, a simple 3-step search mechanism is employed with initial directions chosen as $\theta' = 45^{\circ}$, 50°, 40° along a short segment. The search is continued in the same manner from the end point of that segment where on the magnitude of the integrand has a minimum value.

Numerical evaluation of the integral along each segment is performed using variable with Romberg quadrature [24]. The process continues until the last segment is 10^{-3} of the total sum. The integration is then stopped.

CHAPTER V. THE GAUSSIAN BEAM REPRESENTATIONS

In the conventional Gaussian Beam Method, the fields radiated by the source are stacked along ray paths which serve as trajectories for paraxial Gaussian beams. The paraxial beam fields are computed via the parabolic equation method which yields beam like solutions of wave equation concentrated in the vicinity of these central rays. The total wave field at any observation point is then determined as the discrete superposition of individual Gaussian beams which have traversed the propagation environment on their way from the source to the observer. A major advantage of Gaussian beam method is the use of dynamic ray tracing without regard to transition regions such as caustics [25] and shooting of beams eliminates exhaustive search for the ray paths.

However, the application of the GBM to the inhomogeneous medium [25] revealed that for the chosen parameters such as beam width, number of beams and the width of the cone stacked by beams for a given observation point, starts to fail as the observer moves along the range. This effect is more pronounced as the beams begin to experience more reflections from the boundary depending on the location of the observer. Hence, GBM requires the adjustment of these parameters each time as the observer changes its location.

A. THE COMPLEX SOURCE POINT FIELD

An alternative approach to paraxial beam summation (GBM) is to obtain beam like expressions using Huyghen's principle to continuously distributed source points on a complex initial surface. For numerical implementation, the integration is discretized, each discrete element generates the complete beam solution, without paraxial approximation.

The conventional Gaussian beam method, on the other hand, relies on the paraxial approximation of each complex ray.

To generate an incident Gaussian beam, a z-directed line source with unit strength and suppressed time dependence $e^{+j\omega t}$ is assumed to be located at the complex source point $\tilde{s}$ with coordinates [19]

$$\tilde{x}_0 = x_0 - jb\sin\alpha \ , \ \tilde{y}_0 = y_0 + jb\cos\alpha \qquad b>0 \ , \ y_0>0 \qquad (5\text{-}1)$$

in a complex $(\tilde{x},\tilde{y})$ coordinate space, with the tilde denoting a complex quantity. Interpreted in the real (x,y) coordinate space, b is the beam width parameter, (x_0,y_0) is the location of the beam waist center, and α specifies the direction of the beam axis (see Fig.5).

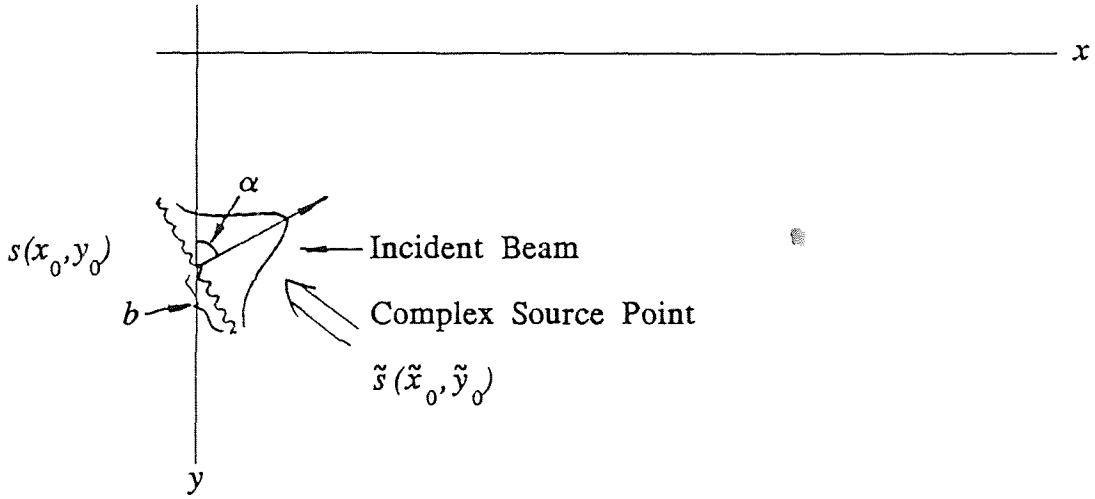

Fig.5. Physical configuration of the complex-source-point representation.

At a real observation point $P(x,y)$ with $x,y>0$, the direct and reflected complex ray fields following (4-1) and (4-2) can be represented respectively as

$$\tilde{G}_1(x,y) = jk^{1/3}\int_{-\infty}^{+\infty} Ai\{k^{2/3}(1+q\tilde{y}_0 - w^2)e^{j\pi/3}\}\ Ai\{k^{2/3}(1+qy-w^2)e^{-j\pi/3}\}$$
$$e^{-jkqw(x-\tilde{x}_0)}\,dw \qquad (5\text{-}2)$$

and

$$\tilde{G}_2(x,y)=j\kappa^{1/3}\int_{-\infty}^{+\infty}\frac{e^{j\pi/3}Ai'\{\kappa^{2/3}(1-w^2)e^{-j\pi/3}\}}{Ai'\{\kappa^{2/3}(1-w^2)e^{j\pi/3}\}}\,Ai\{\kappa^{2/3}(1+q\tilde{y}_0-w^2)e^{j\pi/3}\}$$
$$Ai\{\kappa^{2/3}(1+qy-w^2)e^{j\pi/3}\}\;e^{-jkqw(x-\tilde{x}_0)}\,dw \qquad (5\text{-}3)$$

Again one can evaluate these integrals by numerical integration along steepest descent path or asymptotic methods. The asymptotic evaluation of the complex source point direct ray field in (5-2) is

$$\tilde{G}_1(x,y)\cong\sqrt{\frac{2\pi}{\kappa\,\tilde{Q}_1''(\tilde{w}_{s1})}}\,\tilde{F}_1(\tilde{w}_{s1})e^{-jk\{-2/3(1+q\tilde{y}_0-w^2)^{3/2}+2/3(1+qy-w^2)-qw(x-\tilde{x}_0)\}} \qquad (5\text{-}4)$$

where $\tilde{w}_{s1}$ is the saddle point and is determined from

$$\tilde{Q}_1'(\tilde{w}_{s1})=\{2\tilde{w}_{s1}(1+q\tilde{y}_0-\tilde{w}_{s1}^2)^{1/2}-2\tilde{w}_{s1}(1+qy-\tilde{w}_{s1}^2)^{1/2}-q\tilde{w}_{s1}(x-\tilde{x}_0)\}=0$$

The second derivative of the phase function is

$$\tilde{Q}_1''(w)=\{2(1+q\tilde{y}_0-w^2)^{1/2}-2w^2(1+q\tilde{y}_0-w^2)^{-1/2}\}$$
$$-\{2(1+qy-w^2)^{1/2}-2w^2(1+qy-w^2)^{-1/2}\}$$

and the term in the amplitude is given as

$$\tilde{F}_1(w)=\frac{j}{4\pi\,(1+q\tilde{y}_0-w^2)^{1/4}\,(1+qy-w^2)^{1/4}}$$

Similarly, the reflected complex source point saddle point contribution of the integral in (5-3) is

$$\tilde{G}_2(x,y)\cong$$
$$\sqrt{\frac{2\pi}{\kappa\,\tilde{Q}_2(\tilde{w}_{s2})}}\;\tilde{F}_2(\tilde{w}_{s2})\;\times \qquad (5\text{-}5)$$
$$e^{jk\{-2/3(1+q\tilde{y}_0-w^2)^{3/2}-2/3(1+qy-w^2)^{3/2}+4/3(1-w^2)-qw\,(x-\tilde{x}_0)\}}$$

where $\tilde{w}_{s2}$, the complex saddle point is determined by

$$\tilde{Q}_2'(\tilde{w}_{s2})=\{2\tilde{w}_{s2}(1+q\tilde{y}_0-\tilde{w}_{s2}^2)^{1/2}+2\tilde{w}_{s2}(1+qy-\tilde{w}_{s2}^2)^{1/2}-4\tilde{w}_{s2}(1-\tilde{w}_{s2}^2)^{1/2}-q(x-\tilde{x}_0)\}=0$$

remaining quantities are defined as

$$\tilde{Q}_2''(w)=\{2(1+q\tilde{y}_0-w^2)^{1/2}-2w^2(1+q\tilde{y}_0-w^2)^{-1/2}\}+\{2(1+qy-w^2)$$
$$-2w^2(1+qy-w^2)^{-1/2}\}-\{4(1-w^2)^{1/2}-4w^2(1-w^2)^{-1/2}\}$$

and

$$\tilde{F}_2(w)=\frac{j}{4\pi\ (1+q\tilde{y}_0-w^2)^{1/4}\ (1+qy-w^2)^{1/4}}$$

B. COMPLEX HUYGHEN'S PRINCIPLE - GAUSSIAN BEAM STACKING

To implement the complex Huyghen's synthesis of the field $G(x,y)$ of a real source located at (x_0,y_0), one can consider complex sources to be distributed along a complex cylindrical wavefront with complex radius $(s+jb)$, with s,b real. The location of each complex source is expressed as

$$\tilde{x}_{0\alpha}=x_0-(s+jb)\sin\alpha,\ \tilde{y}_{0\alpha}=y_0+(s+jb)\cos\alpha \qquad 0\le\alpha\le 2\pi \qquad (5\text{-}6)$$

where the surface parameter α is the beam-axis angle measured clockwise from the negative y-axis in real space, s is the radius of the wavefront in real space and b is the beam width parameter as shown in Fig.5. One now can express the real line source field $G(x,y)$ by the complex source distribution, each element of which generates a spectral amplitude $\tilde{\Phi}$

$$G(x,y)=\int_{-\pi}^{+\pi}\tilde{\Phi}\,\tilde{G}(\alpha)d\alpha \qquad (5\text{-}7)$$

The discretized and windowed version for numerical evaluation of (5-7) becomes

$$G(x,y)\cong\sum_{\alpha 1}^{\alpha 2}\tilde{\Phi}\,\tilde{G}(\alpha)\Delta\alpha\ , \qquad -\pi<\alpha_1<\alpha_2<\pi\ ,\ \Delta\alpha\ll 1 \qquad (5\text{-}8)$$

One can see if $b=0$, $\tilde{G}(\alpha)$ takes the form of $\tilde{G}_1(x,y)$ or $\tilde{G}_2(x,y)$ in (5-2) or (5-3). Hence, one can evaluate $\tilde{G}(\alpha)$ in the same way described in section A.

C. EVALUATION OF SPECTRAL AMPLITUDE $\tilde{\Phi}$

By using Gaussian beam stacking algorithm, one must first evaluate the weighting factor $\tilde{\Phi}$ in (5-7) or (5-8). The weighting factor could be determined if one is able to approximate integrals in (5-2) and (5-3)

with their approximate paraxial beam expressions. An alternative approach to evaluate the weighting factor $\tilde{\Phi}$ is to consider numerical integration.

From (5-8) one can get

$$G(x,y) \cong \sum_{\alpha 1}^{\alpha 2} \tilde{\Phi}\, \tilde{G}(\alpha) \Delta\alpha = \tilde{\Phi} \sum_{\alpha 1}^{\alpha 2} \tilde{G}(\alpha) \Delta\alpha$$

Applying (4-3),(4-5) and (5-4),(5-5), one can get

$$G(x,y) = G_1(x,y) + G_2(x,y) \tag{5-9}$$

and

$$\tilde{\Phi} \sum_{\alpha 1}^{\alpha 2} \tilde{G}(\alpha) \Delta\alpha = \tilde{\Phi} \sum_{\alpha 1}^{\alpha 2} \tilde{G}_1(x,y) \Delta\alpha + \tilde{\Phi} \sum_{\alpha 1}^{\alpha 2} \tilde{G}_1(x,y) \Delta\alpha \tag{5-10}$$

Comparison of (5-9) and (5-10) yields

$$\tilde{\Phi} = \frac{G_1(x,y)}{\sum_{\alpha 1}^{\alpha 2} \tilde{G}_1(x,y)} = \frac{G_2(x,y)}{\sum_{\alpha 1}^{\alpha 2} \tilde{G}_2(x,y)} \tag{5-11}$$

Hence, the direct and reflected ray fields can be expressed as stacks of isolated Gaussian beams. The superposition of beams in a given spectral interval replacing the direct ray field field becomes

$$G_1(x,y) \cong \sum_{\alpha 1}^{\alpha 2} \tilde{\Phi}\, \tilde{G}_1(x,y) \Delta\alpha$$

and similar superposition applied to the reflected ray field

$$G_2(x,y) \cong \sum_{\alpha 1}^{\alpha 2} \tilde{\Phi}\, \tilde{G}_2(x,y) \Delta\alpha$$

The Gaussian beams $\tilde{\Phi}\, \tilde{G}_1(x,y)$ and $\tilde{\Phi}\, \tilde{G}_2(x,y)$ weighted with spectral amplitudes corresponding to beam width $(b=1.0\lambda)$ and $(b=3.0\lambda)$ have been evaluated numerically and plotted in Fig.6. The physical parameters are chosen as $x_0=0$, $y_0=1000_{\text{yards}}$, $x=500_{\text{yards}}$, $y=400_{\text{yards}}$, $-100^\circ \le \alpha \le +100^\circ$, $q=1.4650\times 10^{-3}{}_{\text{yards/s}}$, $f=2000_{\text{Hz}}$ and $c_0=1677.3319_{\text{yards/s}}$.

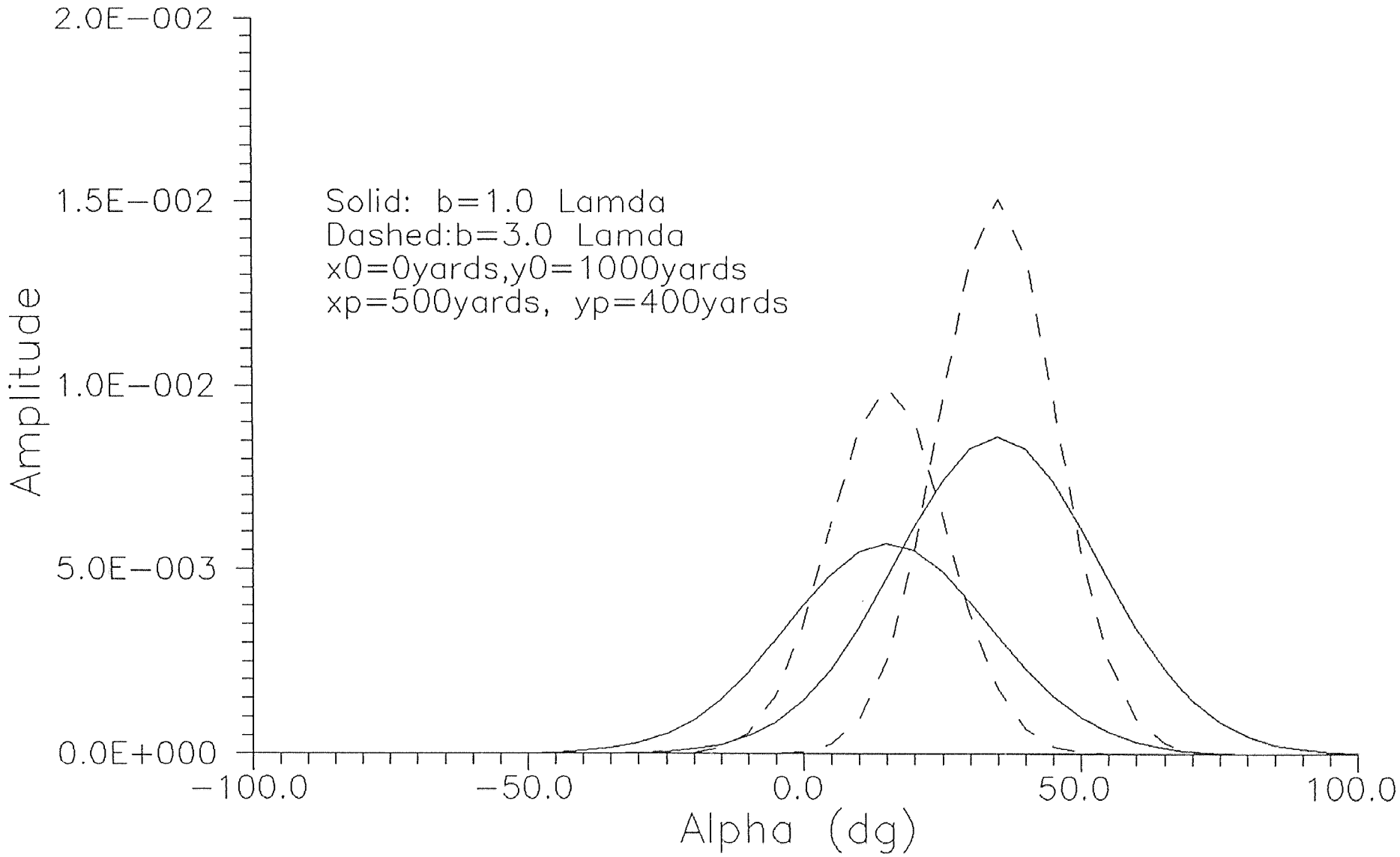

Fig.6 The Gaussian Beams G1(x,y) and G2(x,y) weighed with spectral amplitudes.

CHAPTER VI. NUMERICAL RESULTS

Computer codes have been developed to evaluate the wave fields in the linear profile shown in Fig.1. The methods of evaluation extend from numerical integration to asymptotic evaluation of the ray fields. Saddle points have been determined numerically using falsi regula method. For a real saddle point one has to specify two possible approximate values on both sides of that point to be determined. Hence, the method increments up to a pre-specified accuracy converging on the saddle point. Complex saddle points arising in complex source point method were determined using Newton's method. The initial values for the Newton's method are the corresponding values when the source point is real. Airy functions were evaluated using standard routines that are capable to handle complex arguments.

The reference solution in this thesis is obtained using numerical integration of the generalized ray integral. Detailed explanation has already been presented at the end of Chapter IV. In numerical evaluation, a starting point has been chosen at a pre-determined saddle point. The steepest descent path has been searched. However, knowledge of the saddle point does not guarantee the convergence in numerical integration. A solid line in Fig.7-Fig.11 represent the reference solution. As the observer approaches the shadow boundary, a difficulty was encountered in determination of the steepest descent path and hence for a number of points in range, numerical integration of the Green's function was not computed.

The asymptotic evaluation of the Green's function for real source coordinates was satisfactory up to the shadow boundary. Beyond this

boundary the reflected asymptotic ray contribution disappears. This results in a discontinuity of the total field because of a sudden disappearance of the reflected ray field. The location of this boundary depends on the depth of the observer location. The discontinuity of the physical field across such a boundary is a clear evidence of the deficiency in ART. The continuity has been corrected using paraxial beams by Porter and Bucker [16]. However, in this thesis since a numerical difficulty has been encountered in determining the complex source point contribution due to reflected wave field, this aspect of the problem still requires further effort.

The complex source point evaluation seems to posses validity and could be further employed to resolve the voids of paraxial beams. Though numerically evaluated paraxial beams [16,17] have simplicity in computations, they become inadequate under various circumstances [17]. One such circumstance was a failure in simulating the wave field if a ray will experince more reflections depending on the observer location. Complex source point solutions in that case correspond to rigorous representations and are not expected to fail in such circumstances. Further, numerical testing has to be performed to assess the validity of the complex source point representations under more severe conditions.

The "free" parameters in the complex source point representations are the width of the cone 'D' stacked with beams, 'M' is the number of beams and 'b' is the width of the beam in terms of wavelengths.

For the case of a narrow beam, $b=0.3\lambda$, the magnitude of the Green's function in the region close to the shadow boundary when the source is located at $y_0=1000_{\text{yards}}$ and an observer depth is $y_p=400_{\text{yards}}$, the magnitude of the Green's function is much smaller than the

reference (see Fig.7.1). The positie effect of increasing the number of beams can be observed in Fig.7.2 and Fig.7.3. However, for accurate representation it is more practical to increase the width of the individual beams keeping the number of beams relatively high. This trend could be tracked down through Fig.8.1 to Fig.8.3. The "optimum" beam parameters in Fig.3 are representing the Green's function very accurately. The entire region from the source to the observer have been evaluated and only the transition region have been depicted in Fig.8.3(a) for the magnitude and in Fig.8.3(b) for the phase of the Green's function.

The reference solution starts to fail as the observer approaches the shadow boundary within the transition region. However, the beam summation still is in good agreement with art solution until the boundary beyond which the reflected ray does not exist. The Reflected ray character is clearly apparent in the region before the shadow boundary. Beyond the shadow boundary, the tracking of the reflected wave field contribution was not achieved with the numerical code that has been developed in this thesis. The results presented are only due to the direct ray, which exhibits the progressive wave character. Fig.9.1 to Fig.9.3 show results for much wider beams $b=5.0\lambda$ and with the parameters chosen, the "optimum" parameters even if the frequency has been decreased by a factor of 10, to $f=200$Hz. If the observer location has been changed and moved closer to the boundary, the "optimum" parameter in the complex source point representation may require slight tuning, which is based on observation of the results given in Fig.11. In this figure the observer was kept *50* yards away from the boundary. In all numerical results there was a consistent agreement of the evaluated Green's function by all different methods.

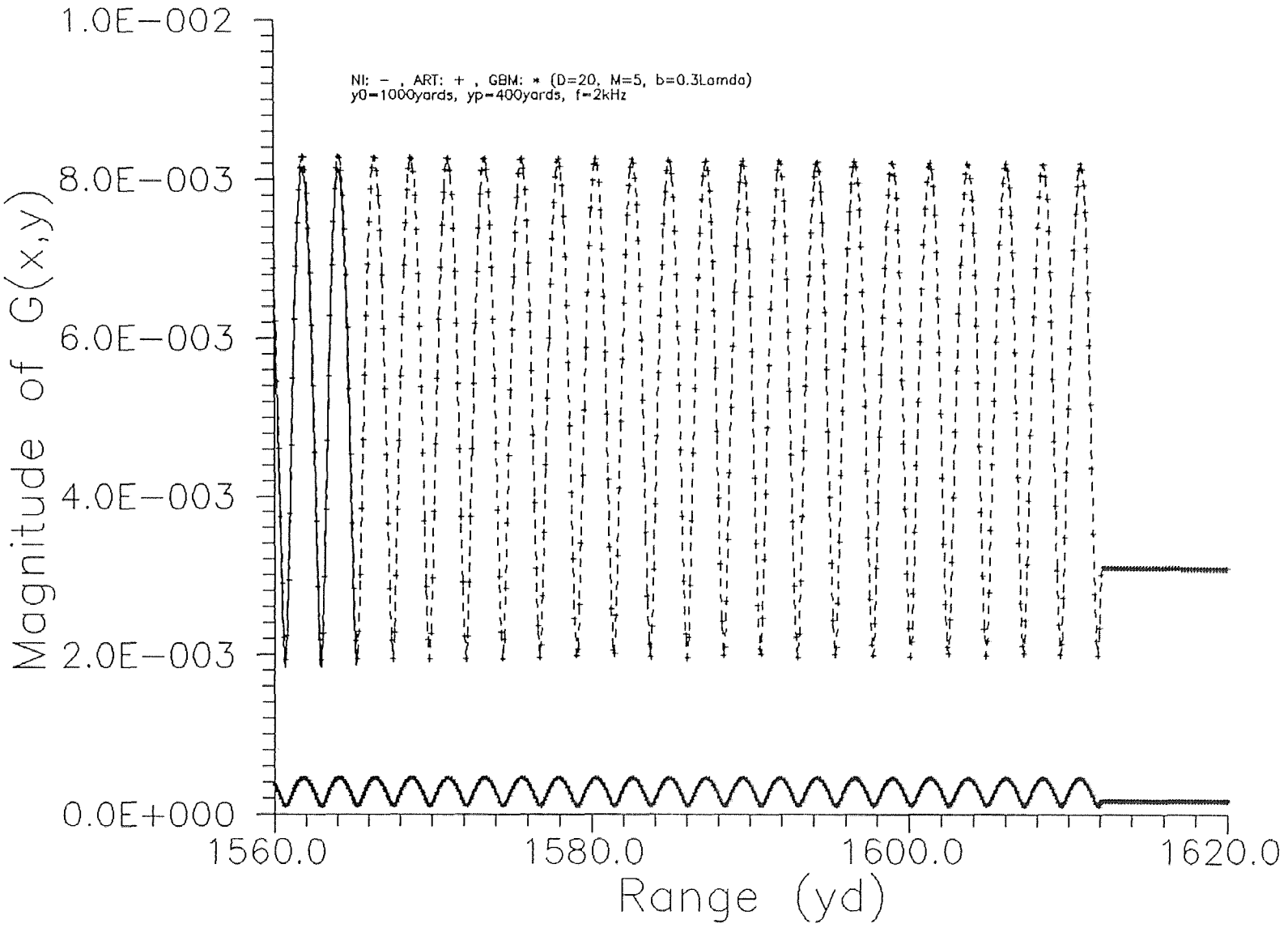

Fig.7.1(a) Magnitude of the Green's funtion versus range.

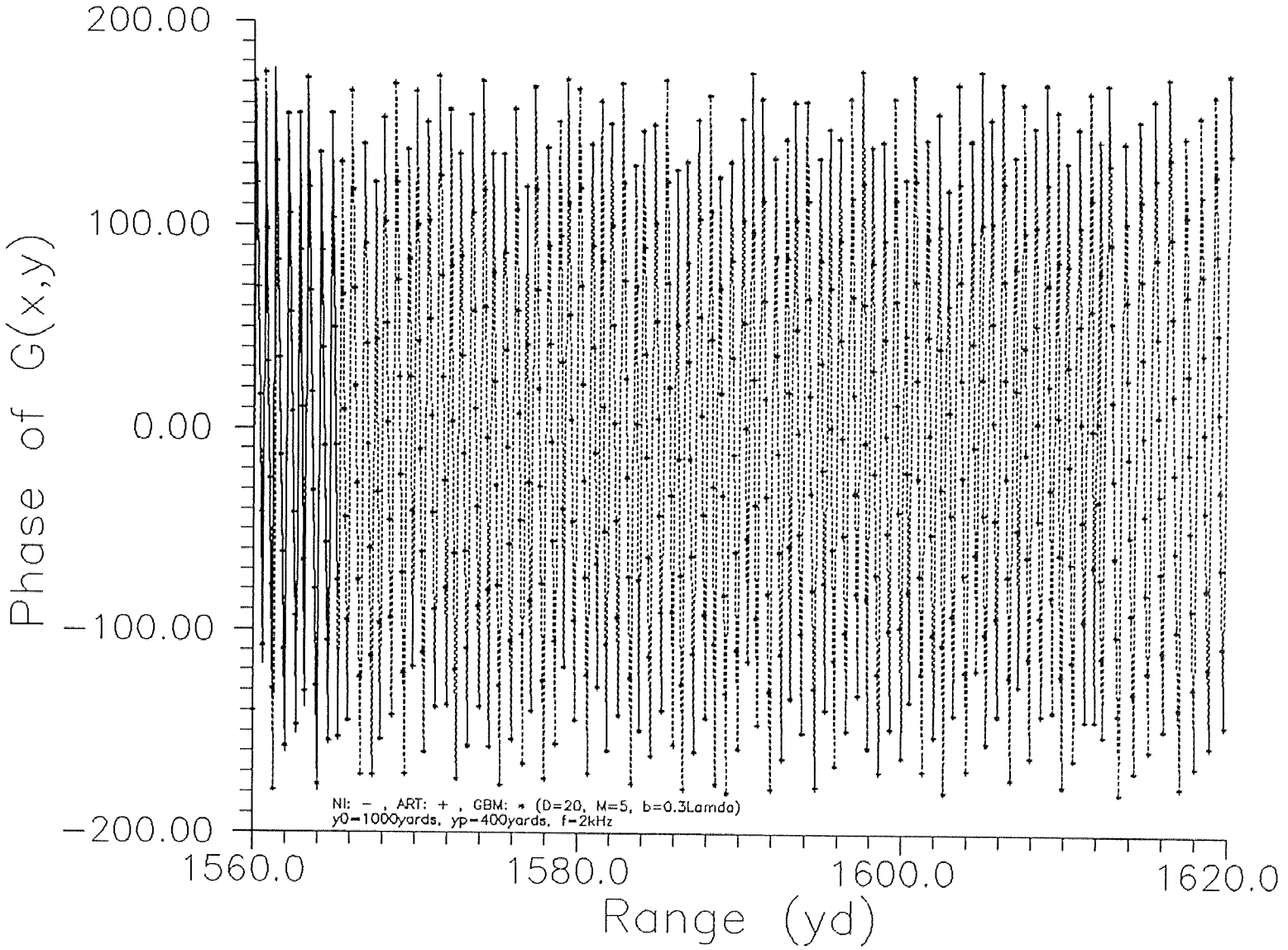

Fig.7.1(b) Phase of the Green's function versus range.

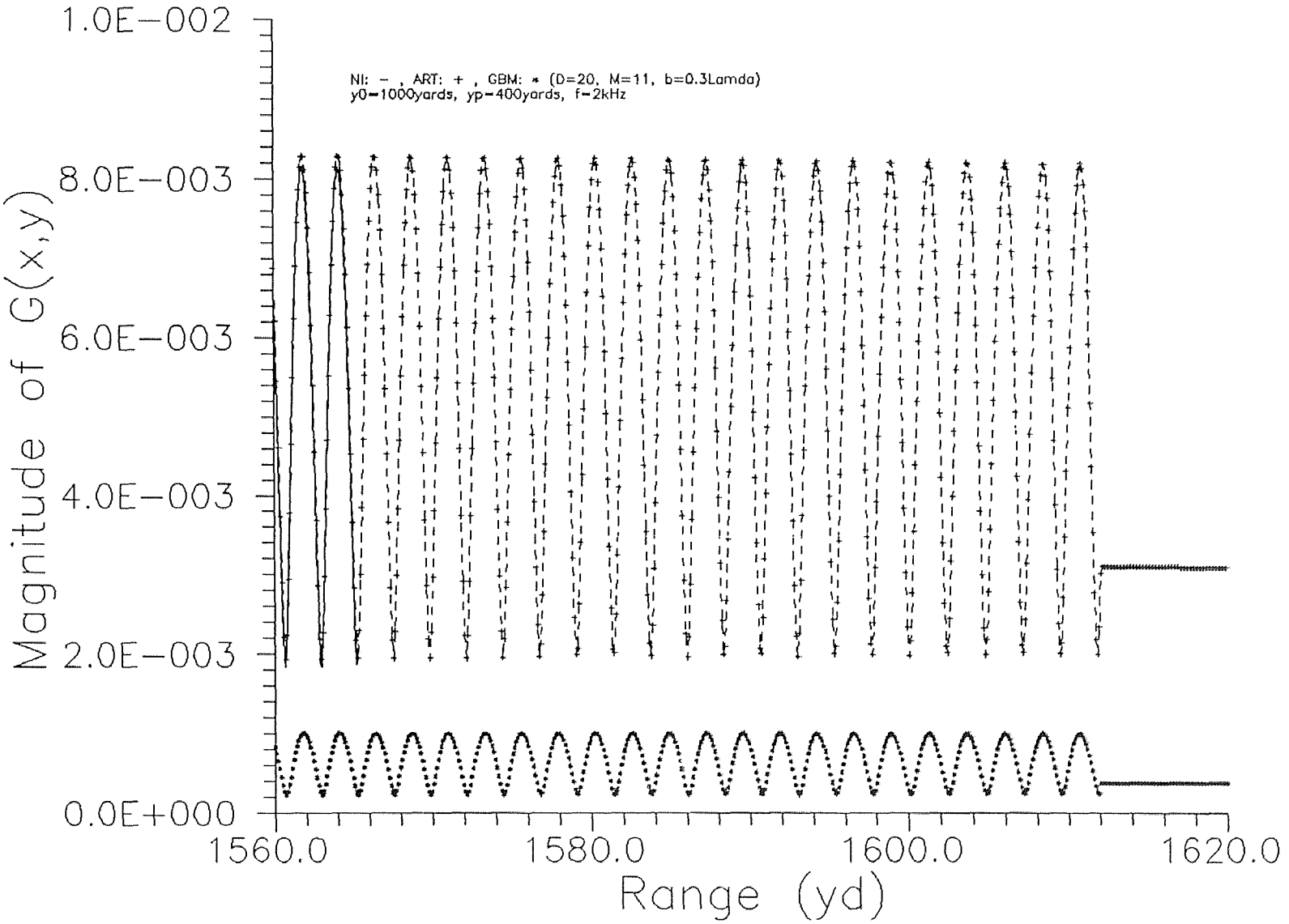

Fig.7.2(a) Magnitude of the Green's funtion versus range.

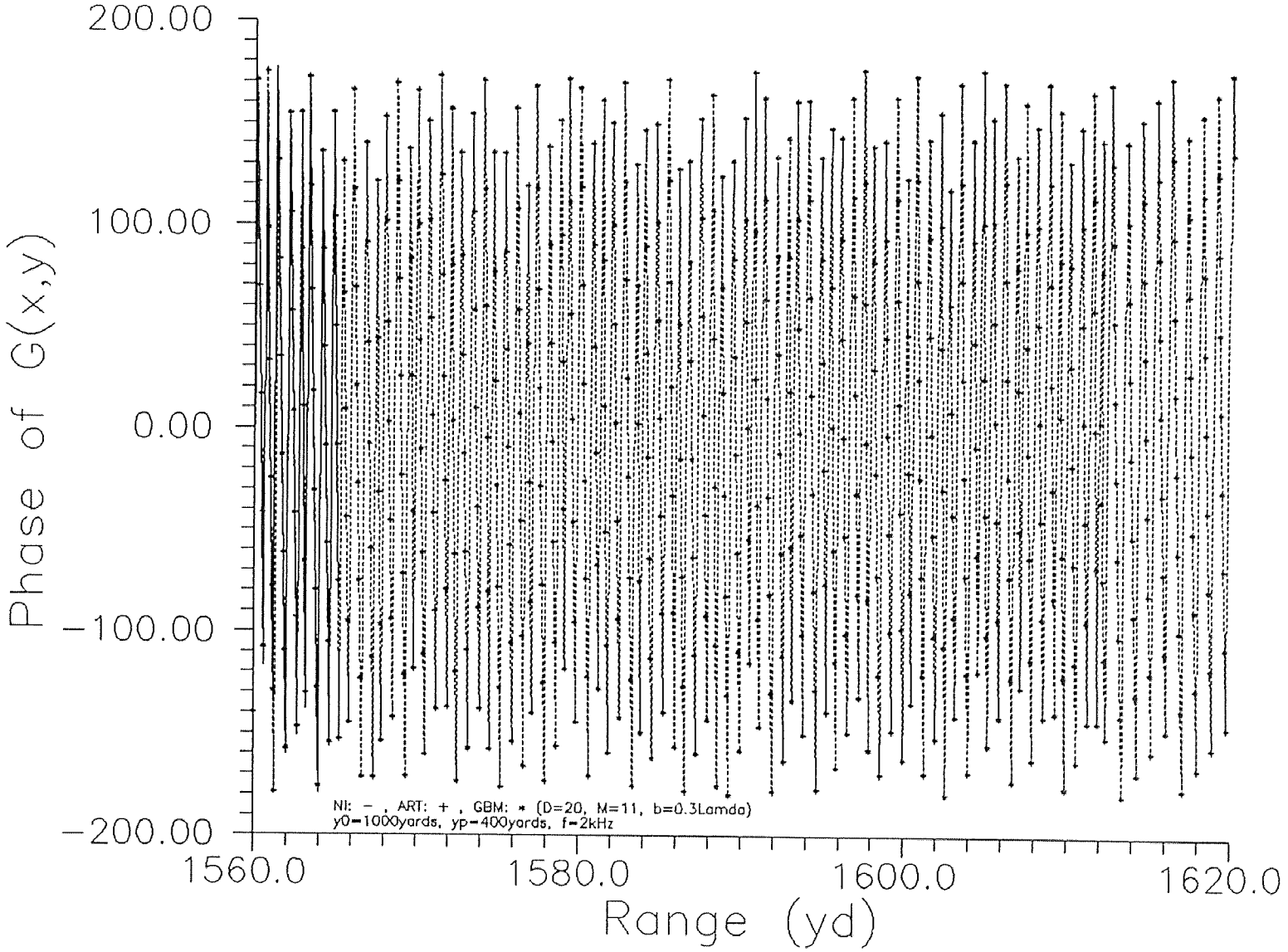

Fig.7.2(b) Phase of the Green's function versus range.

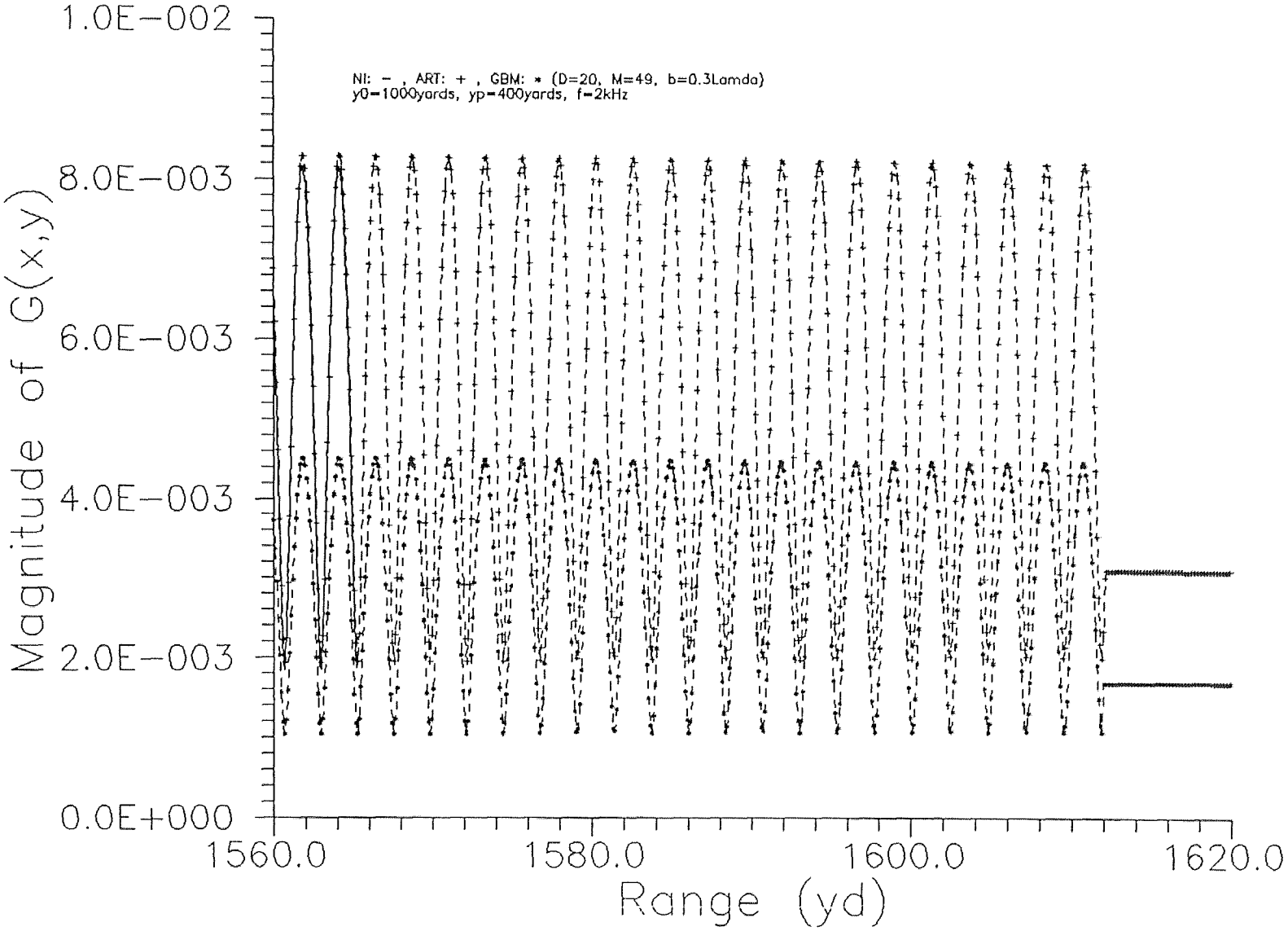

Fig.7.3(a) Magnitude of the Green's funtion versus range.

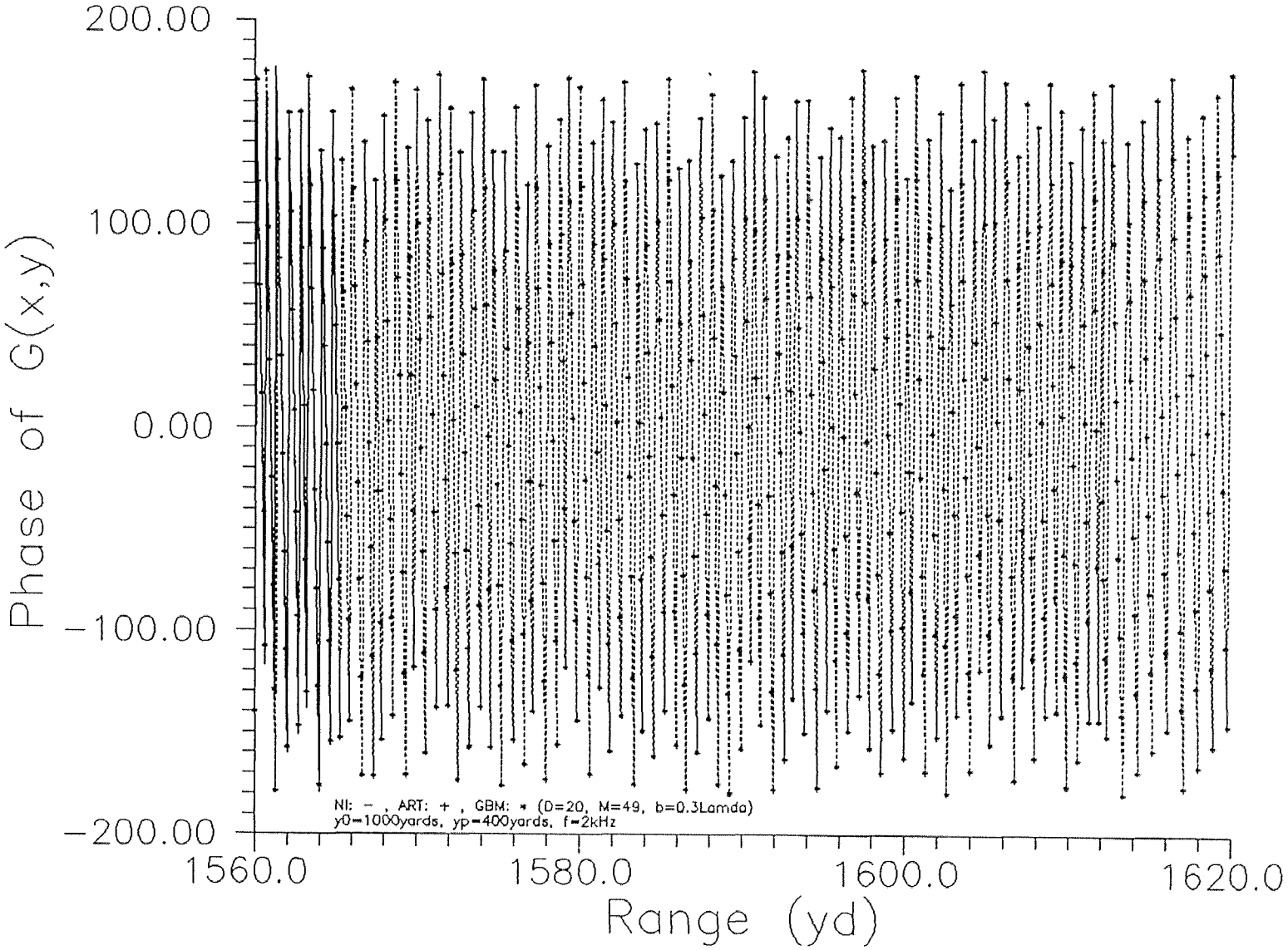

Fig.7.3(b) Phase of the Green's function versus range.

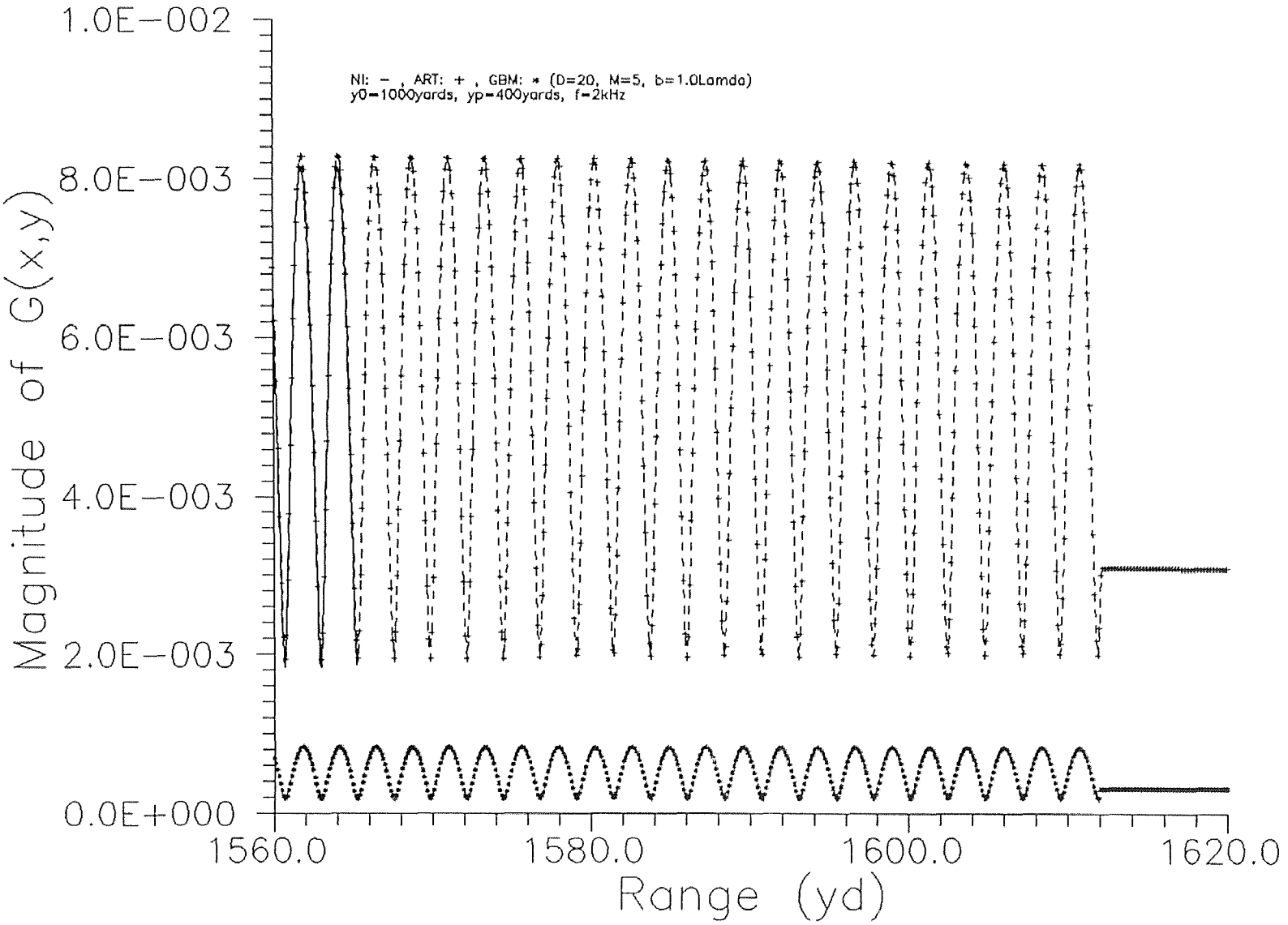

Fig.8.1(a) Magnitude of the Green's funtion versus range.

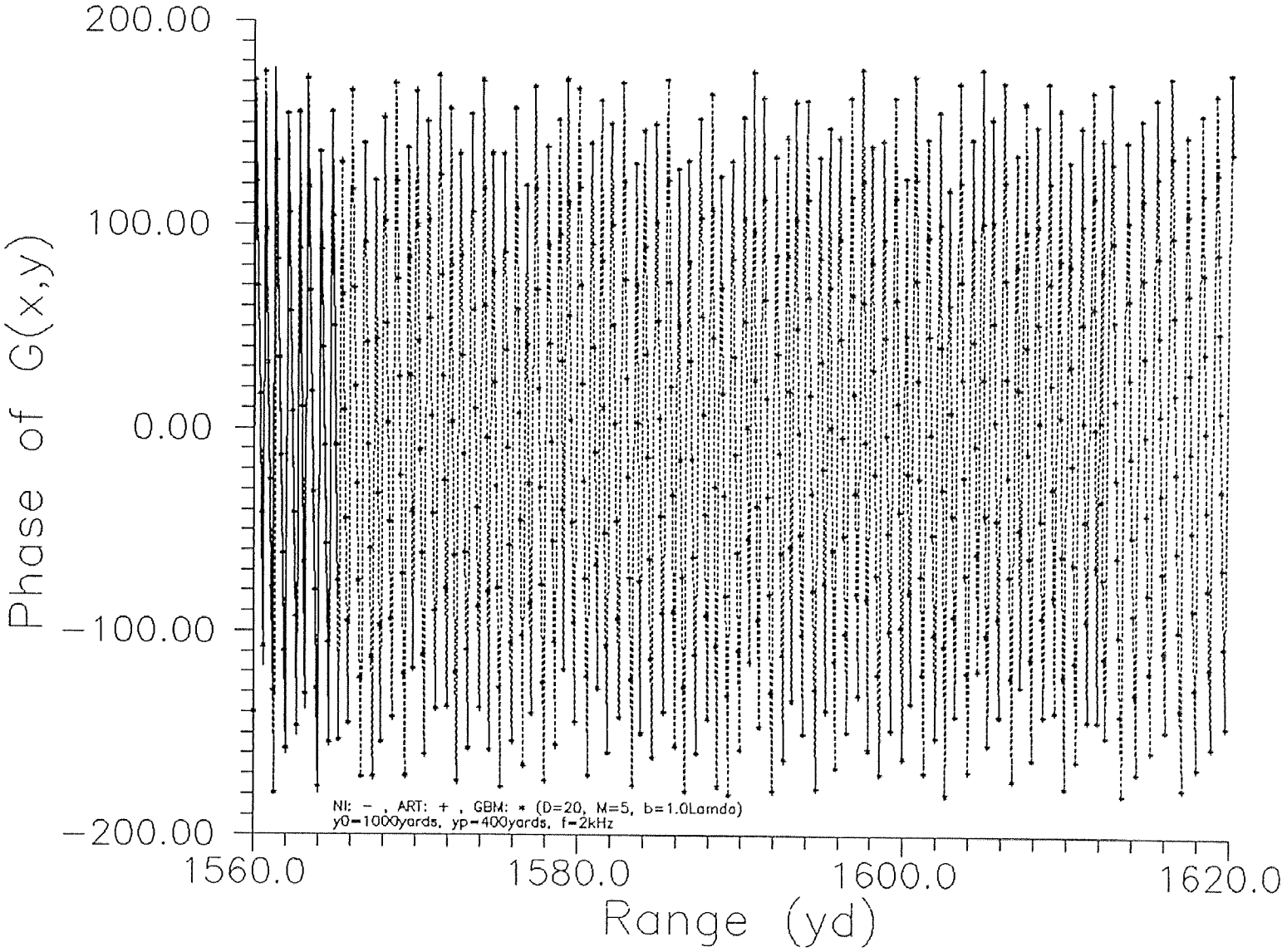

Fig.8.1(b) Phase of the Green's function versus range.

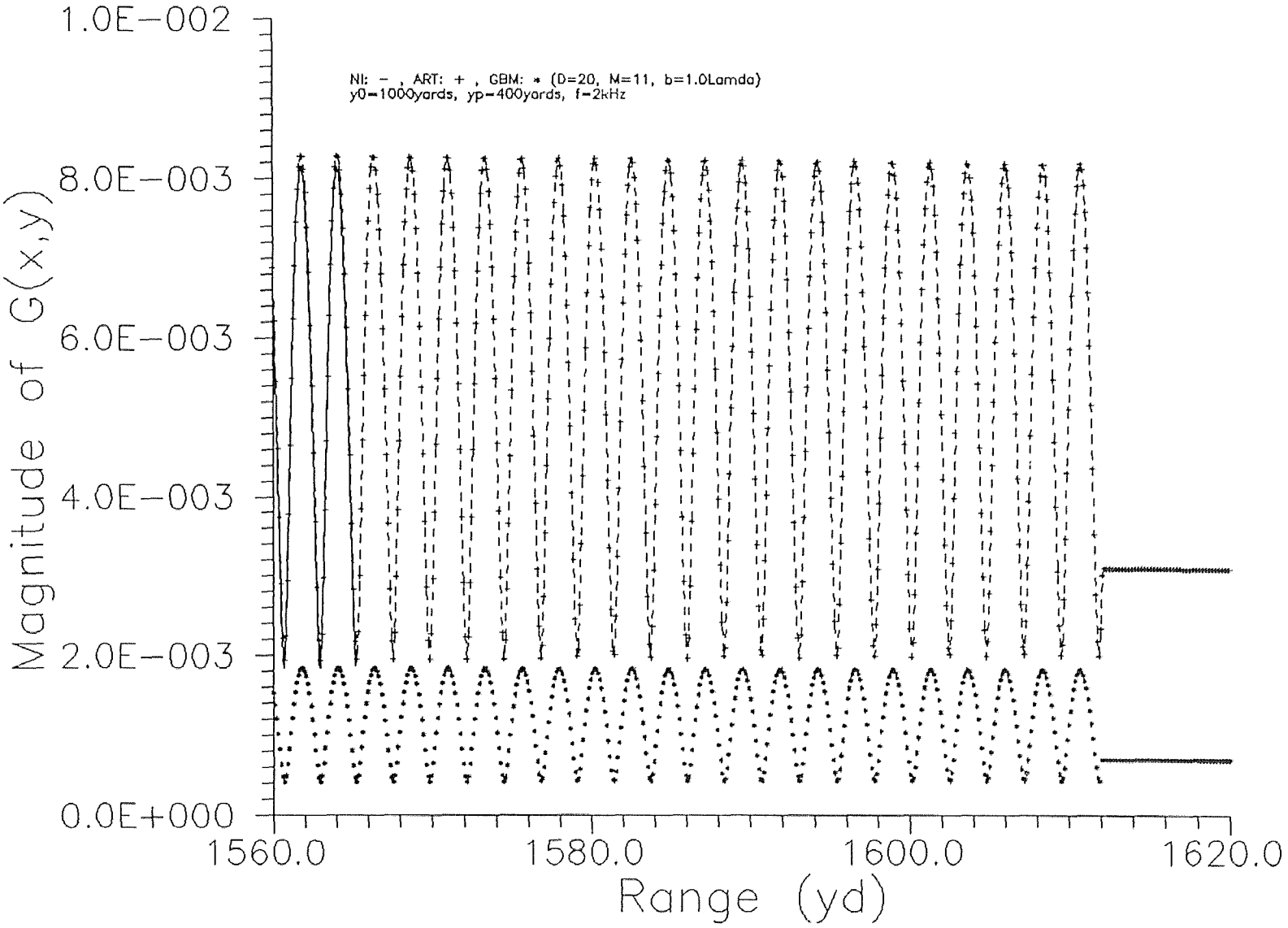

Fig.8.2(a) Magnitude of the Green's funtion versus range.

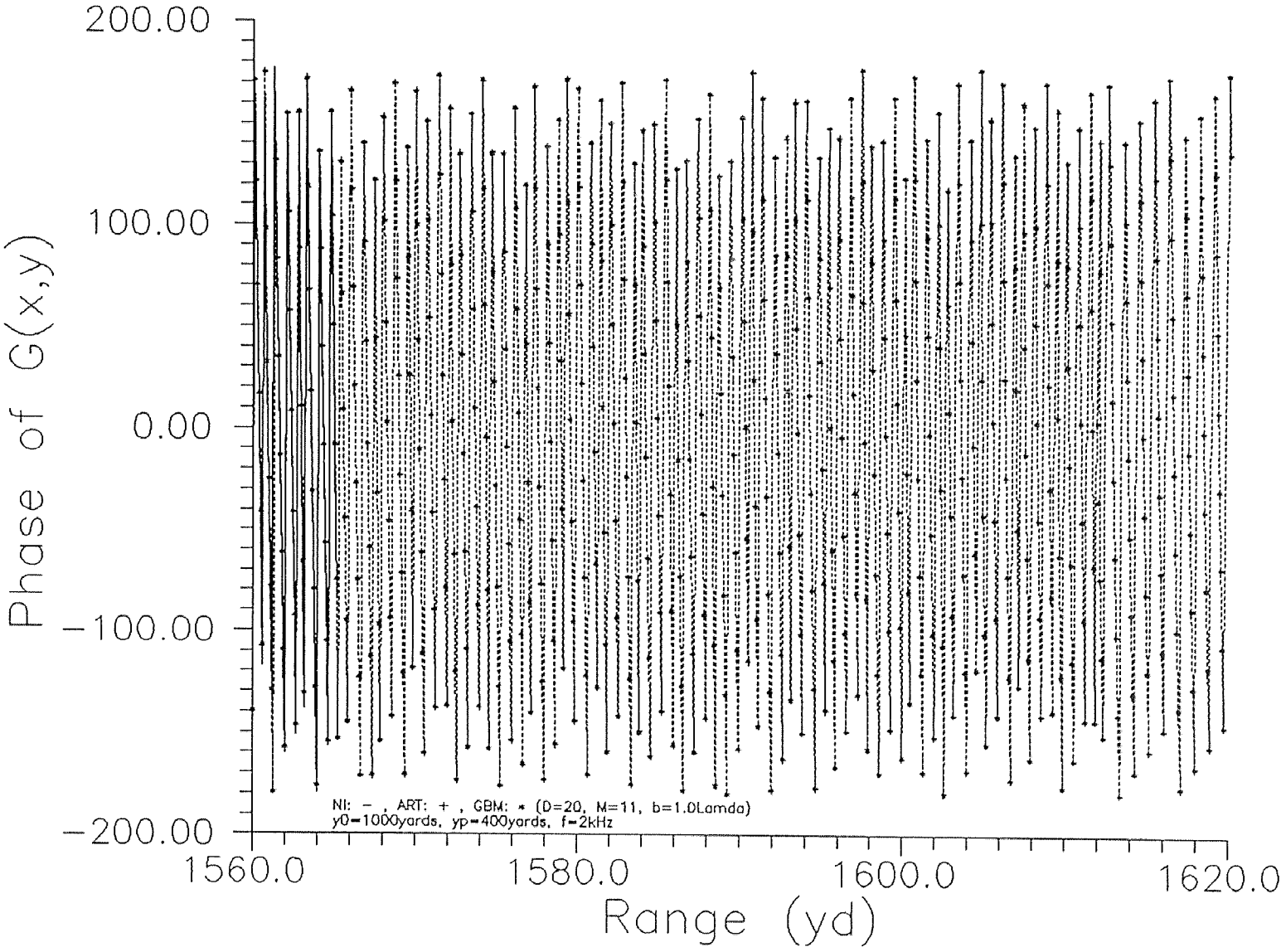

Fig.8.2(b) Phase of the Green's function versus range.

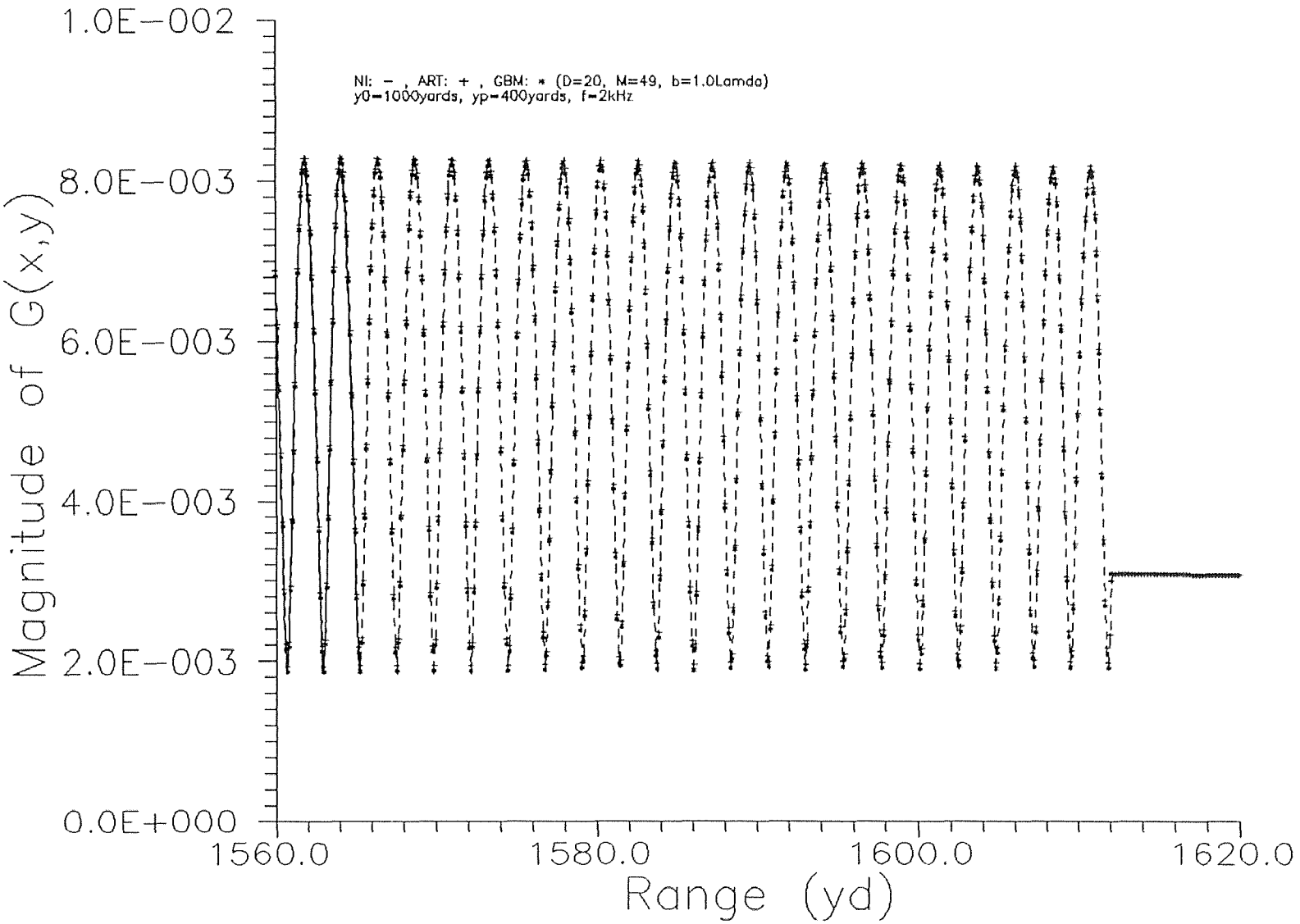

Fig.8.3(a) Magnitude of the Green's funtion versus range.

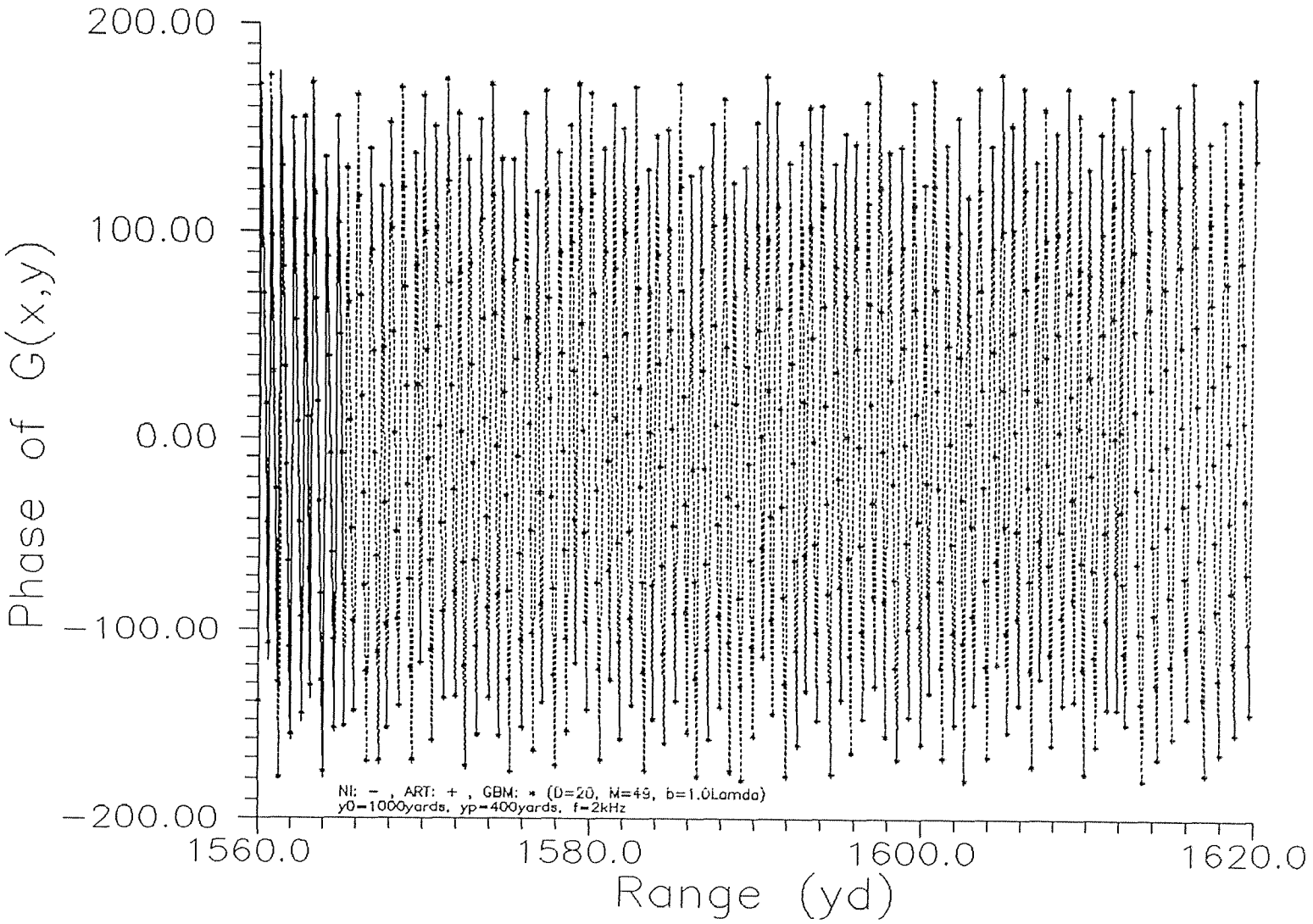

Fig.8.3(b) Phase of the Green's function versus range.

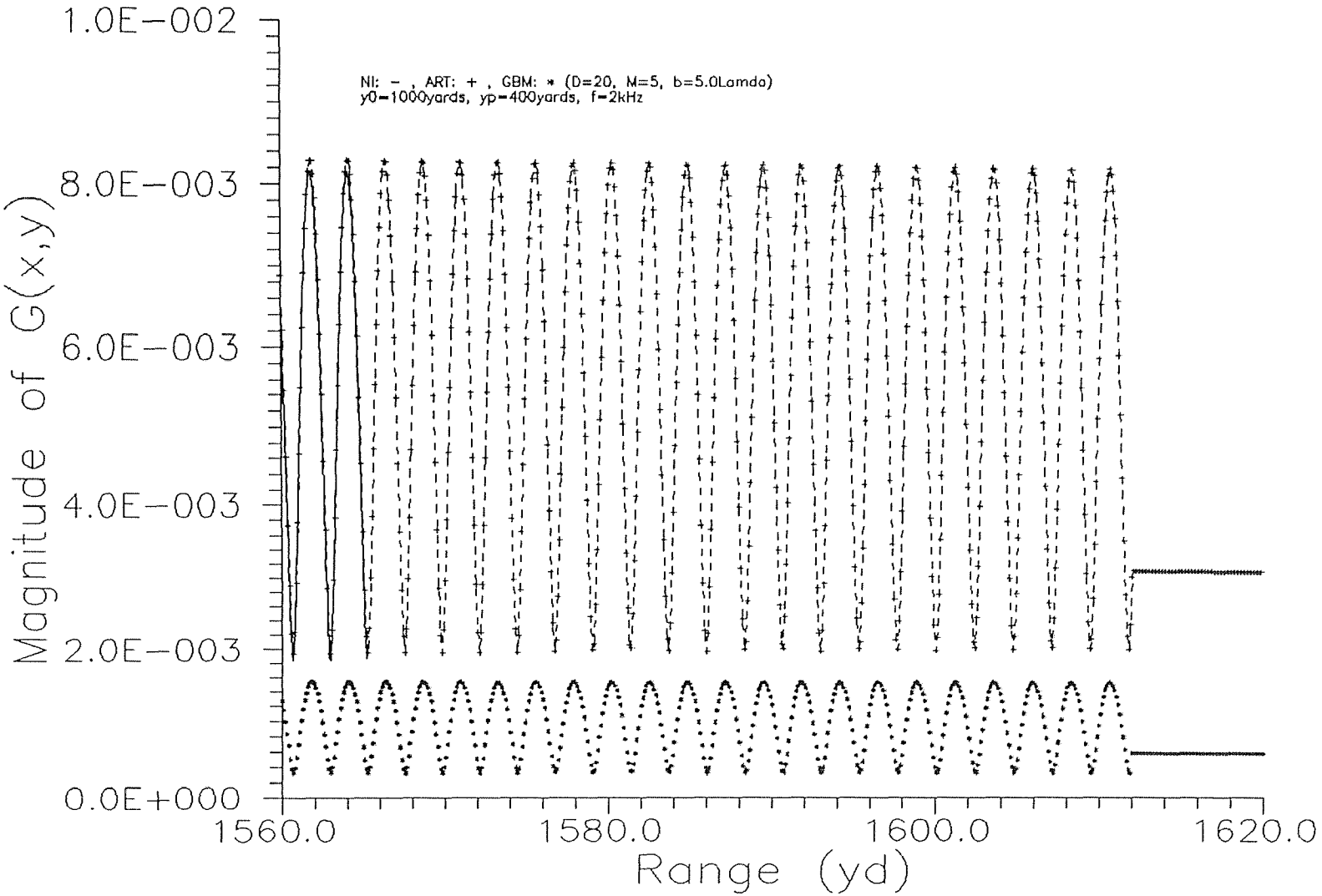

Fig.9.1(a) Magnitude of the Green's funtion versus range.

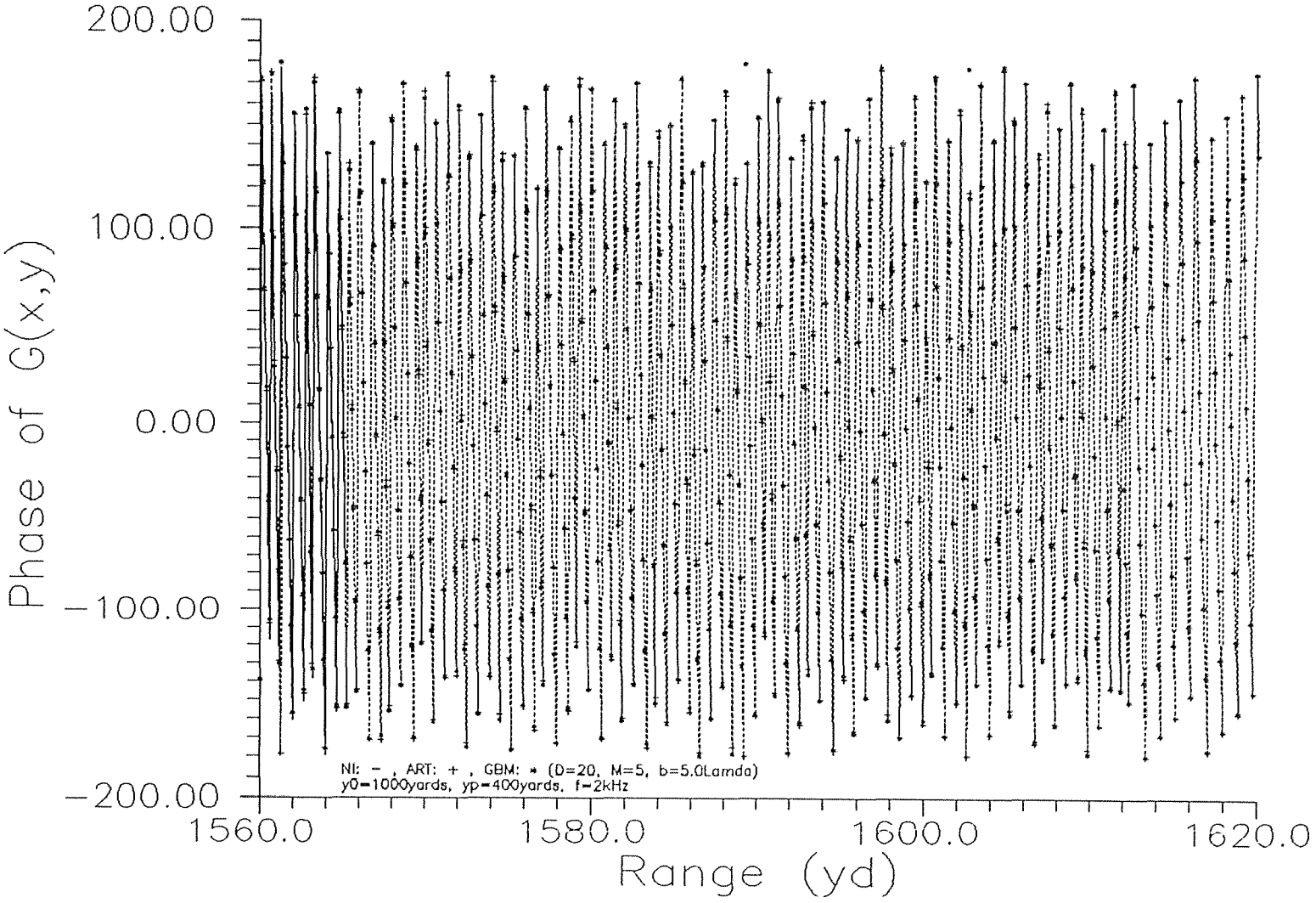

Fig.9.1(b) Phase of the Green's function versus range.

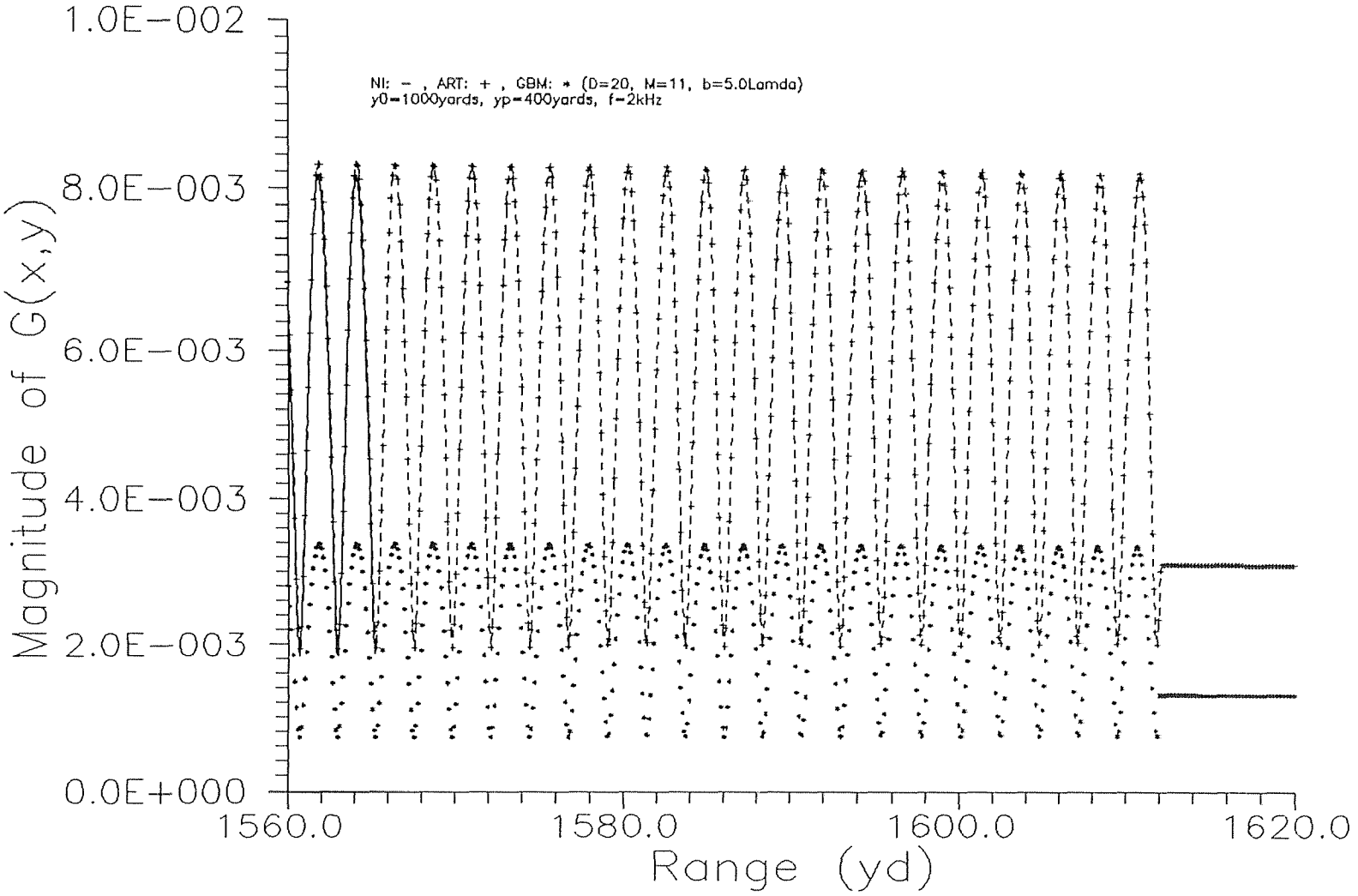

Fig.9.2(a) Magnitude of the Green's funtion versus range.

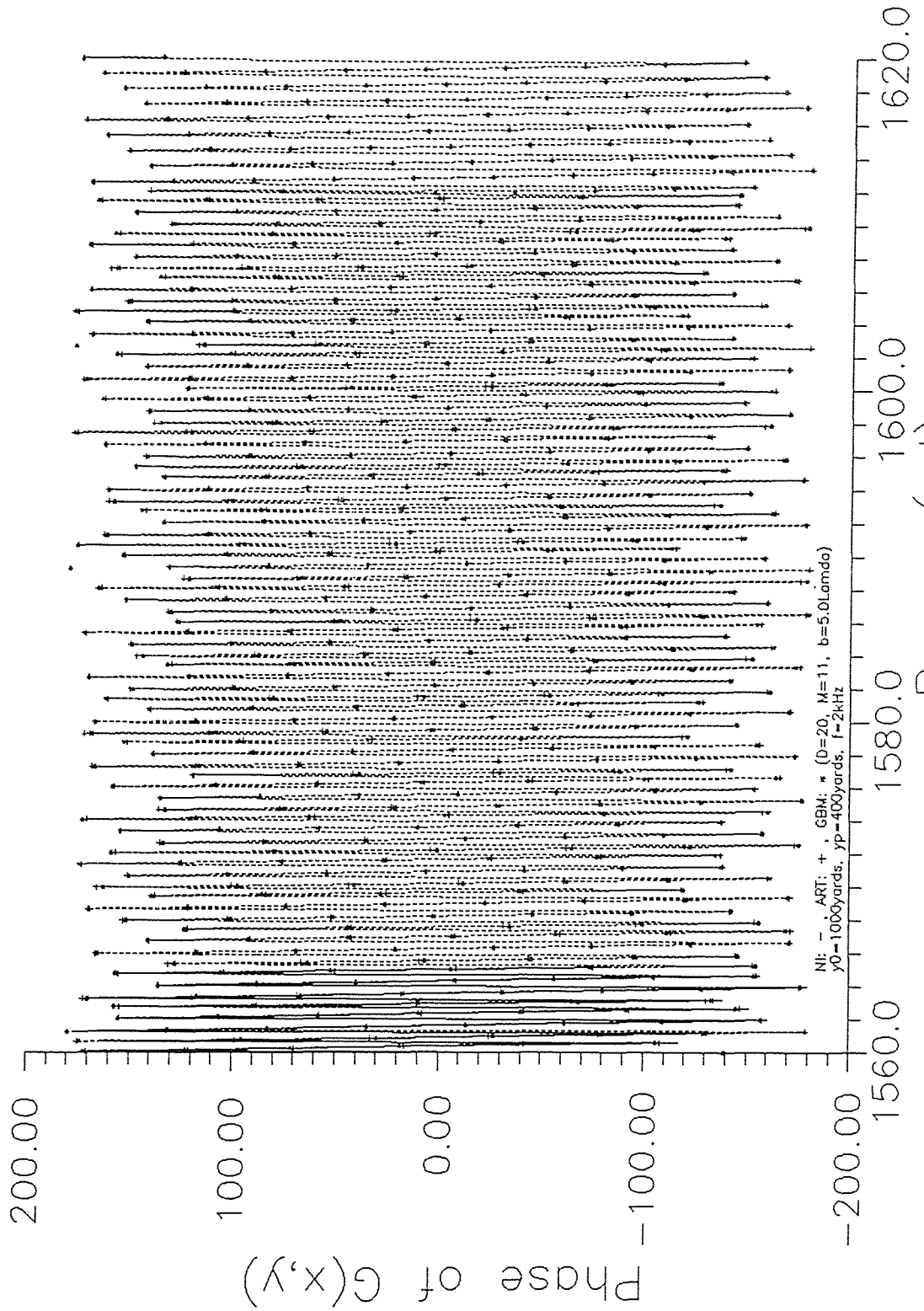

Fig.9.2(b) Phase of the Green's function versus range.

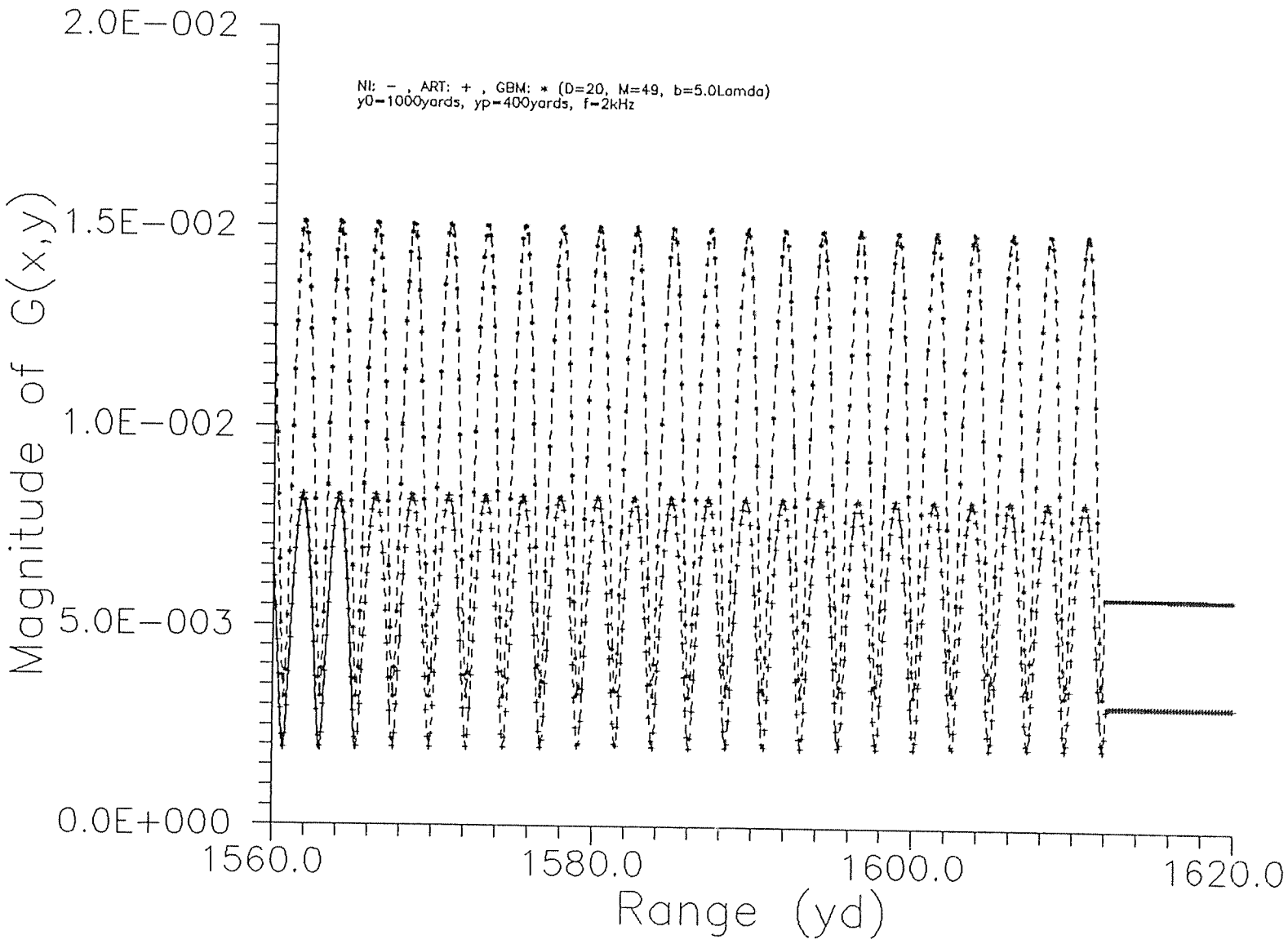

Fig.9.3(a) Magnitude of the Green's funtion versus range.

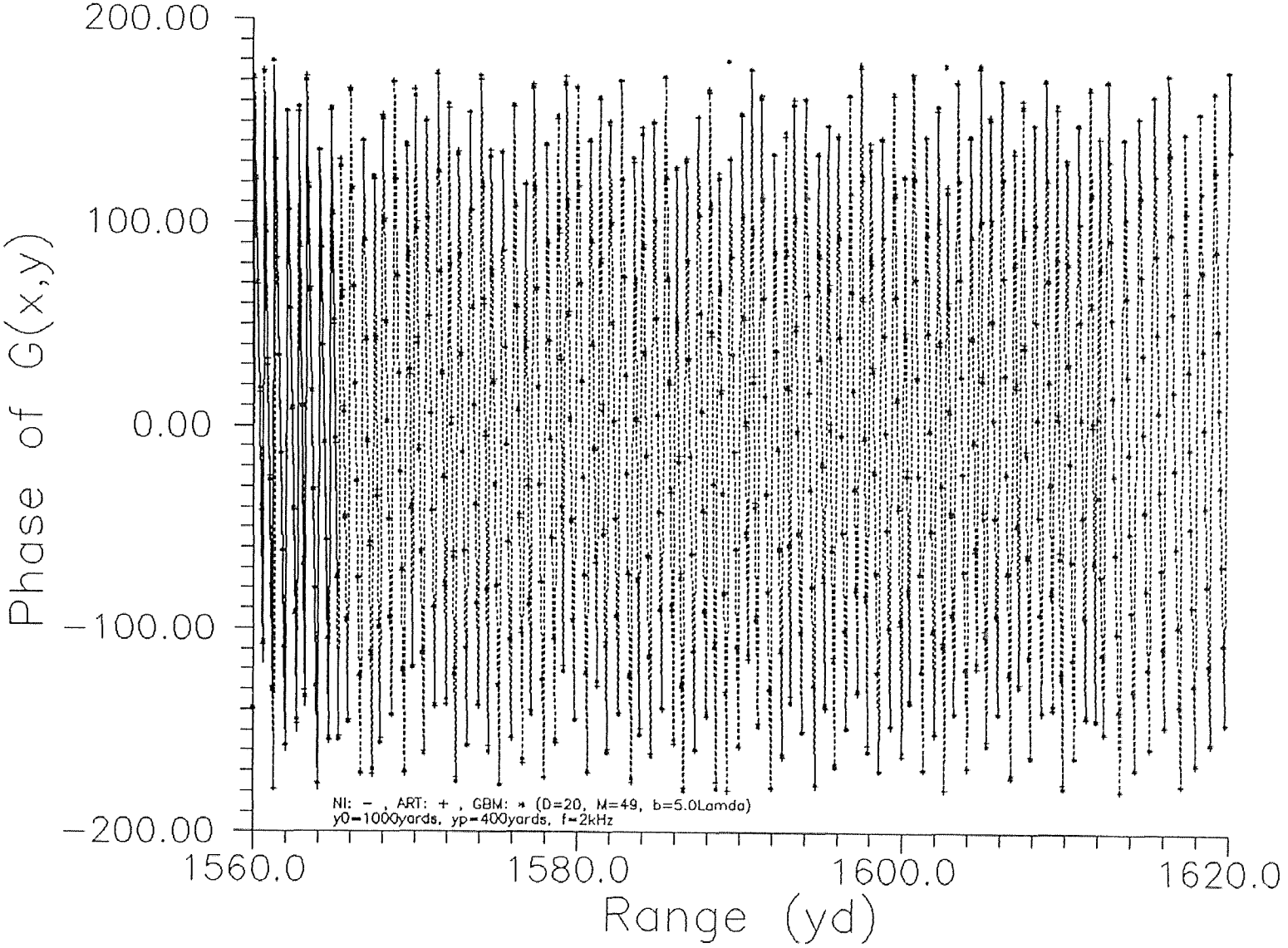

Fig.9.3(b) Phase of the Green's function versus range.

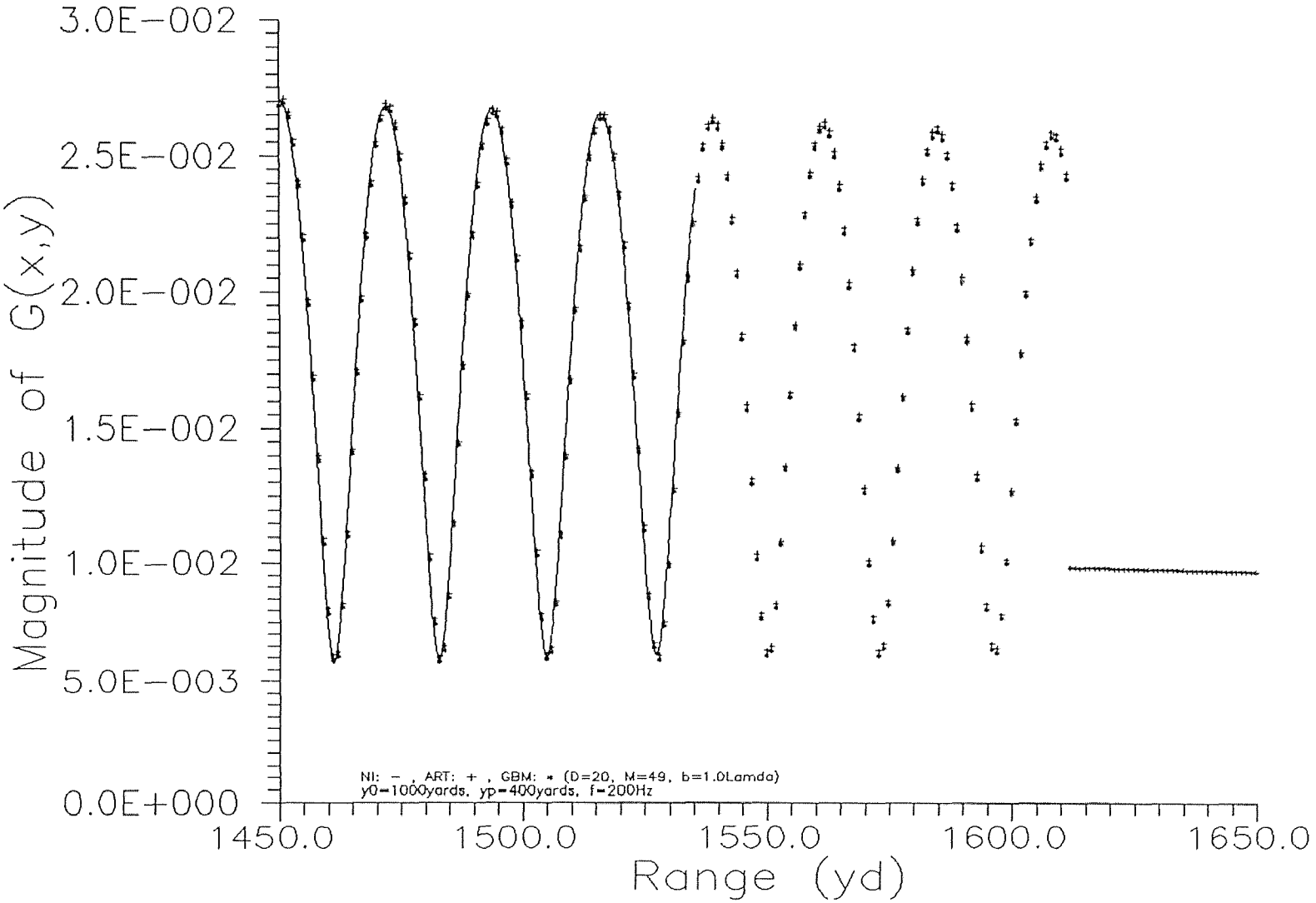

Fig.10(a) Magnitude of the Green's funtion versus range.

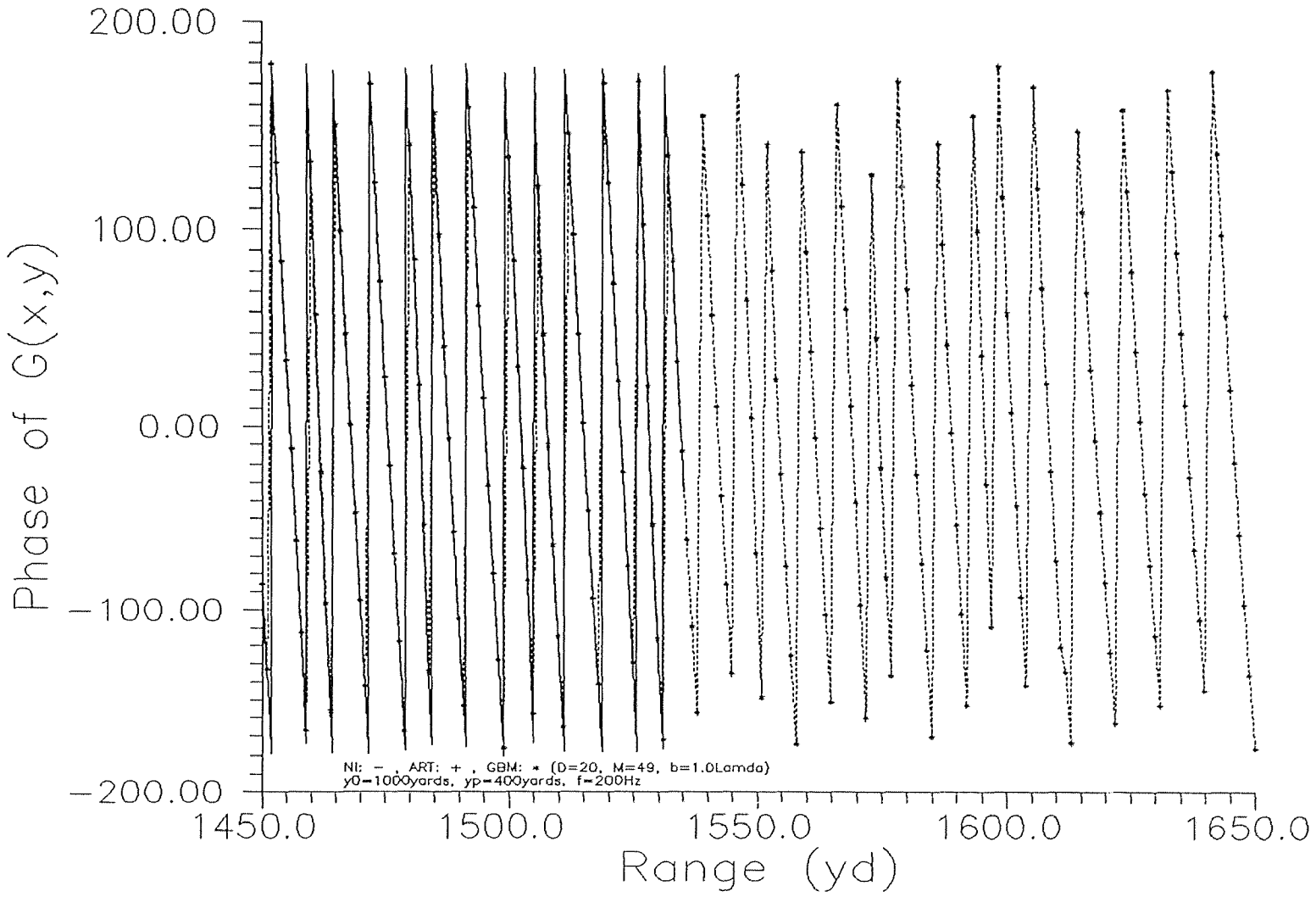

Fig.10(b) Phase of the Green's function versus range.

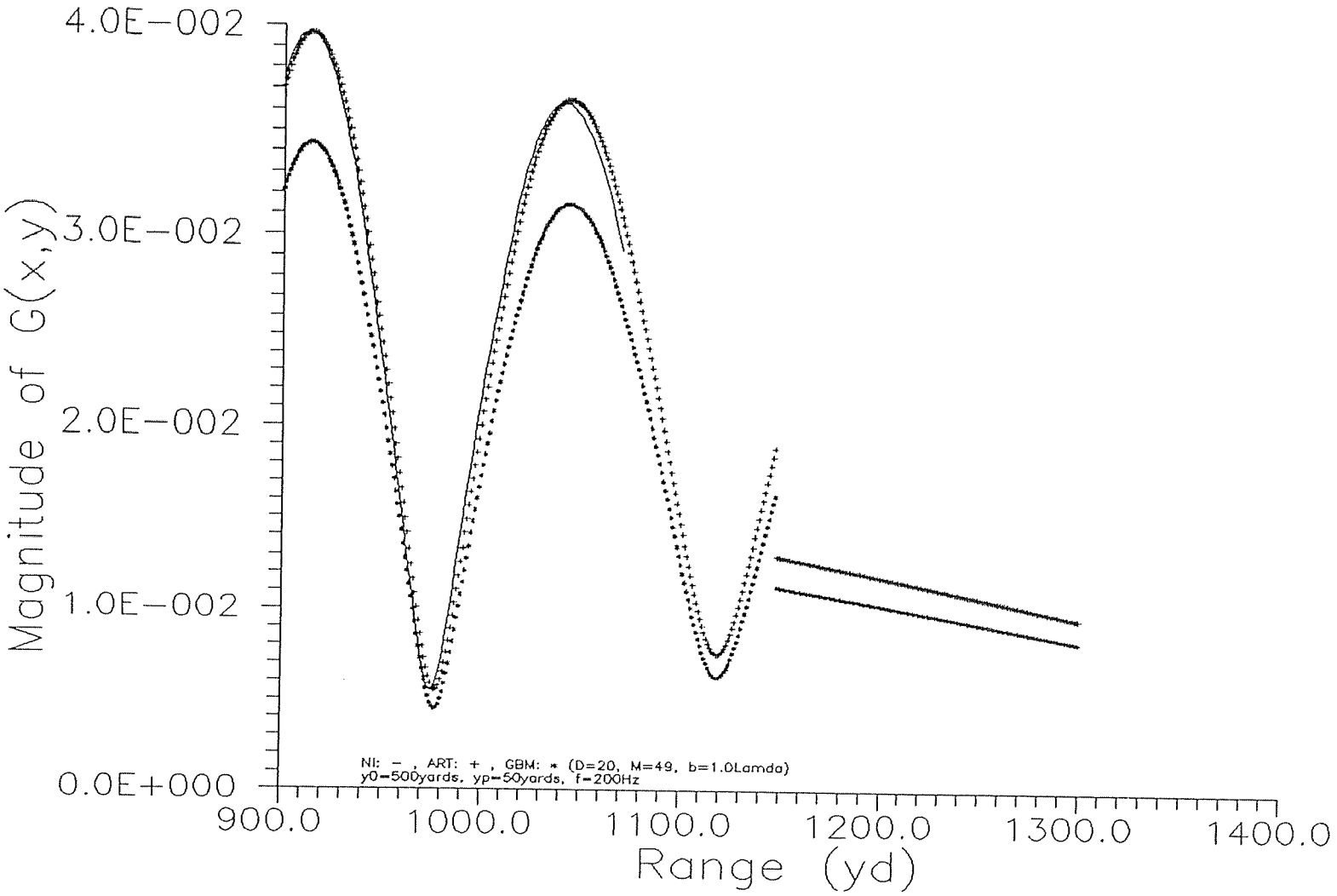

Fig.11(a) Magnitude of the Green's funtion versus range.

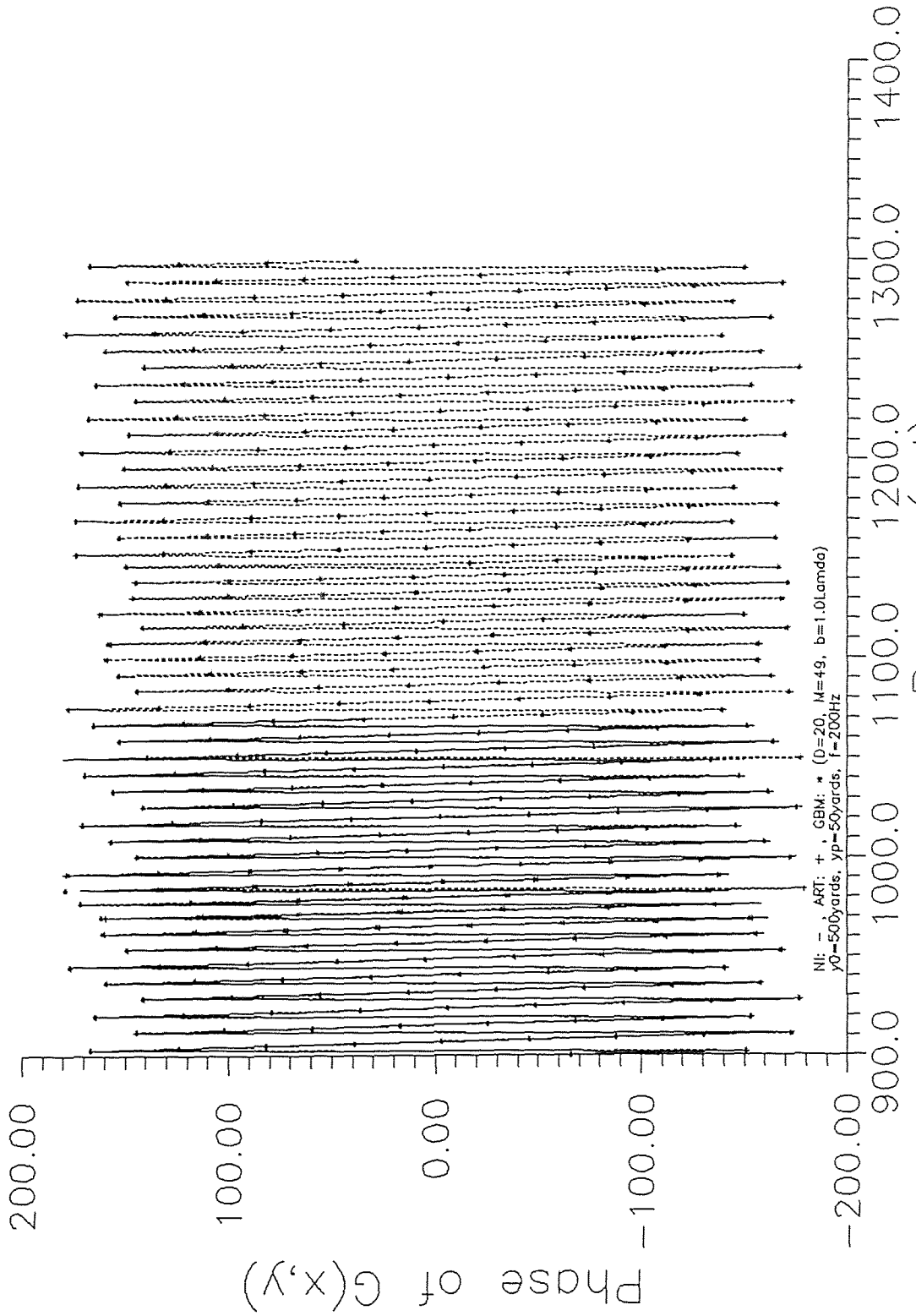

Fig.11(b) Phase of the Green's function versus range.

CHAPTER VII. CONCLUSIONS

The transition region involving the shadow boundary in the linearly increasing refractive region may occur in an anti-duct where on one side of the boundary the field consists of direct and surface reflected contributions while beyond the boundary the asymptotic ray field due to the reflection disappears. Though, the field in the shadow region is not represented in asymptotic ray expression, and discontinuity in the number of rays occurs, its physical effect has to be taken into account. Previous work by Porter and Bucker dealing with paraxial beams has removed this discontinuity and produced a smooth transition. Here, in this thesis an alternative approach using complex source point representation for the beam fields is attempted. Accurate solutions were obtained in terms of summation of complex source generated beams in a wide region between the source and the shadow boundary. However, further work has to be carried out to track the total field through the entire transition region. It had been encountered with a numerical difficulty in determining the steepest descent path for the numerical integration which is used as a reference solution, as the observer was placed in the immediate vicinity of the shadow region. Similar numerical problem arose in determining the complex saddle point due to evanescent wave field contribution. The complex source point approach in general has been successful in tracking the wave field in the inhomogeneous medium. The spectral amplitude factor due to a line source has been determined numerically, though it seems that it will be possible to determine it with an additional analytical effort.

REFERENCES

[1] Felsen, L.B. and Marcuvitz, N., 1973. "Radiation and Scattering of waves", Prentice Hall, New Jersey.

[2] Niver , E., Kamel A. and Felsen L.B. 1984. "Modes to replace transitional asymptotic ray fields in a vertically inhomogeneous earth model", Geophys. J. R. astr Soc. 80, 289-312.

[3] Cerveny, V., Popov ,M.M and Psencik, I.,1981. "Computation of wave fields in inhomogeneous media- Gaussian beam approach", Geophys. J. R. astr. Soc. 70, 109-128.

[4] Cerveny, V., Molotkov, I.A,and Psencik, 1977. "Ray method in seismology", Karlova Univerzita, Praha.

[5] Leontonovich, M.A. and Fock, V.A.,1946. "Solution of the problem of propagation of electromagnetic waves along the earth's surface using parabolic wave equation method", ZETF, 16, 557-573 (in Russian).

[6] Tappert, F.D.,1978. "The parabolic approximation method in Wave propagation and underwater Acoustics", Lecture notes in physics, 70,224-287 ,Springer-Verlag, Berlin.

[7] Claerbout, J.F., 1976. "Fundamentals of Geophysical Data processing", Mc Graw-Hill, New York.

[8] Babich, V.M.,1968. "Eigenfunctions, concentrated in the vicinity of closed geodesics" in Mathematical Problems of Theory of propagation of waves,Vol.9,pp 15- 63,Nauka,Leningrad (in Russian).

[9] Babich, V.M., and Buldyrev, V.S., 1972. "Asymptotic Methods in Problems of diffraction of short waves",Nauka,Moscow (in Russian).

[10] Babich, V.M. and Kirpichnikova ,N.J.,1974. "Boundary Layer method in diffraction problems",Leningrad University Press (in Russian, English translation by Springer-Verlag,1980).

[11] Babich , V.M. and Pankratova ,T.F.,1973. "On discontinuities of the Green function of mixed problem for wave equation with variable coefficients", in Problems of mathematical physics, Vol.6, pp.9-27, Leningrad University Press (in Russian).

[12] Popov, M.M,1981. "A new method of computation of wave fields in the high frequency approximation", Preprint LOMI AN SSSR,E-I-81,Leningrad.

[13] Cerveny , V. and Psencik, I. 1982. "Gaussian beams in two dimensional elastic inhomogeneous media", Geophys. J. R. astr. Soc. (1983) 72,417-433.

[14] Nowack, R.,and Aki K. "The 2-d gaussian beam synthetic method testing and application", 1984, Geophys. J. R. astr. Soc. Vol.89, pp.1466-94

[15] Yomogida, K. "Gaussian beams for surface waves in Laterally Slowly Varying Media", 1984, Geophys. J. R. astr. Soc. published.

[16] Porter, M.B. and Bucker, H.P., 1987. "Gaussian beam tracing for computing ocean acoustic fields", J. Acoust. Soc. Am. , Vol.82(4), pp.1349-59.

[17] Niver, E., Ruiz, C.J., Vogas, M.S. and Felsen, L.B., 1987. "Critical test of Gaussian beam method for multiply reflected fields in a surface duct", 113 Acoustical Society Meeting, Indianapolis, (J. Acoust. Soc. Am., Supplement 1, Vol. 81, p.S9).

[18] Deschamps, G.A., 1971. "Gaussian beam as a bundle of complex rays", Elec. Lett., 7(23), pp.684-5.

[19] Felsen, L.B., 1984. " Geometrical theory of diffraction evanescent waves, complex rays and Gaussian beams", J. R. Astr. Soc., 79, pp.77-88.

[20] Lu, I.T., Felsen, L.B. and Ruan, Y.Z., 1987. "Spectral aspects of the Gaussian beam method: reflection from a homogeneous half-space", Geophys. J. R. Soc. (1987) 89, pp.915-932.

[21] Pedersen, M.A. and Gordon, D.F., 1972. "Normal-mode and ray theory applied to underwarter acoustic conditions of extreme downward refraction", J. Acoust. Sco. Am. 51, pp.323-368.

[22] Jones, D.S., 1963. "High-frequency refraction and diffraction in general media", Philosop. Transactions of Royal Soc., Vol.255, A.1058, pp.341-387.

[23] Abramowitz, M. and Stegun, I.A., 1970. "Handbook of Mathematical functions", Dover, NY.

[24] Miller, E.K., 1970. "A variable interval width quardrature technique bases on Romberg's Method", J. of Copmp. hys., Vol.9, pp.265-279.

[25] Niver, E., Vogas, M.S., and Felsen, L.B., 1986. "Correcting ray field failures caused by focusing in an inhomogeneous duct: a critical look at the Gaussian beam method", AGARD Conference Proceedings No.407, pp.10.1-10.11.